Threatscapes for the aeroconservation of birds

Sergio A. Cabrera-Cruz[1], Scott R. Loss[2], Jeffrey J. Buler[3], Emily B. Cohen[4]

[1] Unidad de Servicios Profesionales Altamente Especializados, Instituto de Ecología A. C., Xalapa, Veracruz, Mexico

[2] Department of Natural Resource Ecology and Management, Oklahoma State University, Stillwater, Oklahoma, USA.

[3] Department of Entomology and Wildlife Ecology, University of Delaware, Newark, Delaware, USA.

[4] University of Maryland Center for Environmental Science, Appalachian Laboratory, Frostburg, Maryland, USA.

Abstract:

The airspace is increasingly cluttered with threats to aerial organisms in the form of anthropogenic structures and vehicles, likely contributing to bird population declines through additive mortality mediated by collisions. In the United States alone, up to and likely exceeding one billion birds die annually due to collisions aloft, and most of these fatalities are related to six threat types: aircraft, buildings, communication towers, power lines, roads, and wind turbines. Collisions happen where birds and threats co-occur; hence, identifying where aerial threats are is a first step in determining avian exposure to risk of collision. Here, we present two collections of high-resolution (30 m) maps that we collectively refer to as *threatscapes*, illustrating the distribution and magnitude of potential impact for the top six sources of anthropogenic bird collision mortality throughout the contiguous United States. The first collection, the *individual-threat maps*, contains 285 state-wide spatial rasters, one for each individual aerial threat type present in each state and the District of Columbia, noting that not all threat types were present in every state. The second collection, the *cumulative-threat maps*, contains 49 spatial rasters displaying the cumulative aerial threat present in each state. To create these threatscapes, we obtained public geospatial data with the distribution of each threat type across the country, and we created risk areas for each individual threat, defined as the two-dimensional spatial footprint where birds may come into contact with structures or vehicles, or where birds may need to take evasive action to avoid colliding with them. We first generated the state-wide *individual-threat maps*, by assigning to individual risk areas of every state the expected annual bird mortality according to threat-specific published estimates, while also accounting for factors affecting variability of mortality within threat type. Then we created the *cumulative-threat maps*, by summing the threat-specific maps of each state. Our threatscapes are meant to provide indices of the negative impact that collision threats have on birds and do not represent actual estimates of expected mortality in any given location. We anticipate that these threatscapes will be useful tools for multiple stakeholders to identify priority locations for conservation. For example, one or more *individual-threat maps* can be combined with bird distribution data to assess avian exposure to risk of collisions with those specific threats, and the *cumulative-threat maps* can be merged with bird abundance data to identify locations where threats may be contributing to avian population declines. Additionally, both types of threatscapes could be used in combination with geospatial data on widespread sensory pollution agents—for example, artificial light at night, which is linked to bird collisions with several types of structures—to identify areas with interactive effects on birds. Furthermore, these high-resolution threatscapes could facilitate analyzing the impact of anthropogenic obstacles on bird movement, or the response of birds to aerial habitat fragmentation. Overall, these datasets will contribute towards research aimed at identifying drivers of bird population change and toward conservation efforts seeking to slow and reverse the ongoing and worsening decline of North American bird populations.

Key words/phrases: aerial habitat, aeroconservation, aeroecology, anthropogenic mortality, anthropogenic threats, avian conservation, bird collisions, bird migration, bird mortality, collision risk, migratory birds.

Open Research: The complete data set is available as Supporting Information at: [to be completed at proof stage]. Associated data is also available at [name of data repository]: [DOI assigned to deposited

material].

* Corresponding Author E-mail: sergio.cabrera@inecol.mx

INTRODUCTION

The lower airspace, an important aerial habitat used by birds and other volant organisms (Diehl 2013, Diehl et al. 2017, Nilsson et al. 2025), is increasingly cluttered with anthropogenic structures and vehicles (Lambertucci et al. 2015). In the United States alone, up to and likely exceeding one billion birds die annually due to collisions aloft, and most of these fatalities are related to six threat types: aircraft, buildings, communication towers, power lines, roads, and wind turbines (Loss et al. 2015).

Bird collisions with structures and vehicles have been documented for over a century, beginning almost as soon as these anthropogenic threats first encroached upon or traversed the airspace (Coues 1876, Stoner 1925, 1936, Spiker 1927, White 1927, Townsend 1931, Rogers et al. 1977, Sodhi 2002, McKee et al. 2016). Collisions can only happen where birds and threats co-occur; hence, identifying the locations of aerial threats is a first step in determining avian exposure to risk of collision with them.

Here, we present two collections of high-resolution (30 m) maps that we collectively refer to as *threatscapes*, illustrating the distribution and magnitude of potential impact for the top six sources of anthropogenic bird collision mortality throughout the contiguous United States.

The term "threatscape" was adopted by ecologists to move beyond single threats (like a single building) toward "landscape level" threats (Leu et al 2008). A threatscape can then be derived from the spatial overlay of hazards over a broad extent. To create our bird-collision-specific threatscapes, we obtained comprehensive public geospatial data with the distribution of each threat type across the contiguous United States, and we created risk areas for each individual threat. We defined risk areas as the two-dimensional spatial footprint where birds may come into contact with structures or moving vehicles, or where birds may need to take evasive action to avoid colliding with these threats. Furthermore, as a measure of potential impact of threats on birds, we assigned to each individual risk area the expected annual bird mortality according to threat-specific published estimates, while also accounting for factors affecting variability of mortality within threat type. Thus, we created bird-collision risk areas around each individual airport, building, communication tower, power line, road, and wind turbine in the country, each with a quantitative measure of its potential negative impact on birds.

The first collection of threatscapes, the *individual-threat maps*, contains 285 state-wide spatial rasters, one for each individual aerial threat type present in each state and the District of Columbia, so that each map displays the potential impact of a threat in a state. While 294 individual-threat maps would be expected given the number of threat types considered (n = 6) and the number of states (48 contiguous, plus DC), not all threats are present in each state (e.g. no wind development in the District of Columbia); hence, the 285 individual-threat maps. The second collection, the *cumulative-threat maps*, contains 49 spatial rasters displaying the cumulative aerial threat present in each state.

These threatscapes can be combined with bird distribution data (e.g. Fink et al. 2022) to assess avian exposure to risk of collision, with other layers of widespread sensory pollution (e.g. Li et al. 2020) that create a compounded negative effect on birds when interacting with collision-related threats (Winger et al. 2019, Van Doren et al. 2021, Nemes et al. 2023), or with movement data to analyze how birds react to aerial habitat fragmentation (Davy et al. 2017), for example through least-cost path analyses or landscape connectivity analyses (e.g. Korpach et al. 2022).

These threatscapes will contribute towards research aimed at identifying drivers of bird population change and toward conservation efforts seeking to slow and reverse the ongoing and worsening decline of North American bird populations (Rosenberg et al. 2019, Johnston et al. 2025).

METADATA

CLASS I. DATA SET DESCRIPTORS

A. Data set identity:

Threatscapes for the aeroconservation of birds

B. Data set identification code:

individual_threatscapes.zip

cumulative_threatscapes.zip

C. Data set description

1. Originators:

a. Sergio A. Cabrera-Cruz. Unidad de Servicios Profesionales Altamente Especializados, Instituto de Ecología A. C., Xalapa, Veracruz, Mexico.

b. Emily B. Cohen. University of Maryland Center for Environmental Science, Appalachian Laboratory, Frostburg, Maryland, United States.

c. Scott R. Loss. Department of Natural Resource Ecology and Management, Oklahoma State University, Stillwater, Oklahoma, United States.

d. Jeffrey J. Buler. Department of Entomology and Wildlife Ecology, University of Delaware, Newark, Delaware, United States.

2. Abstract: The airspace is increasingly cluttered with threats to aerial organisms in the form of anthropogenic structures and vehicles, likely contributing to bird

population declines through additive mortality mediated by collisions. In the United States alone, up to and likely exceeding one billion birds die annually due to collisions aloft, and most of these fatalities are related to six threat types: aircraft, buildings, communication towers, power lines, roads, and wind turbines. Collisions happen where birds and threats co-occur; hence, identifying where aerial threats are is a first step in determining avian exposure to risk of collision. Here, we present two collections of high-resolution (30 m) maps that we collectively refer to as threatscapes, illustrating the distribution and magnitude of potential impact for the top six sources of anthropogenic bird collision mortality throughout the contiguous United States. The first collection, the individual-threat maps, contains 285 state-wide spatial rasters, one for each individual aerial threat type present in each state and the District of Columbia, noting that not all threat types were present in every state. The second collection, the cumulative-threat maps, contains 49 spatial rasters displaying the cumulative aerial threat present in each state. To create these threatscapes, we obtained public geospatial data with the distribution of each threat type across the country, and we created risk areas for each individual threat, defined as the two-dimensional spatial footprint where birds may come into contact with structures or vehicles, or where birds may need to take evasive action to avoid colliding with them. We first generated the state-wide individual-threat maps, by assigning to individual risk areas of every state the expected annual bird mortality according to threat-specific published estimates, while also accounting for factors affecting variability of mortality within threat type. Then we created the cumulative-threat maps, by summing the threat-specific maps of each state. Our threatscapes are meant to provide indices of the negative impact that collision threats have on birds and do not represent actual estimates of expected mortality in any given location. We anticipate that these threatscapes will be useful tools for multiple stakeholders to identify priority locations for conservation. For example, one or more individual-threat maps can be combined with bird distribution data to assess avian exposure to risk of collisions with those specific threats, and the cumulative-threat maps can be merged with bird abundance data to identify locations where threats may be contributing to avian population declines. Additionally, both types of threatscapes could be used in combination with geospatial data on widespread sensory pollution agents—for example, artificial light at night, which is linked to bird collisions with several types of structures—to identify areas with interactive effects on birds. Furthermore, these high-resolution threatscapes could facilitate analyzing the impact of anthropogenic obstacles on bird movement, or the response of birds to aerial habitat fragmentation. Overall, these datasets will contribute towards research aimed at identifying drivers of bird population change and toward conservation efforts seeking to slow and reverse the ongoing and worsening decline of North American bird populations.

D. Key words/phrases:

aerial habitat, aeroconservation, aeroecology, anthropogenic mortality, anthropogenic threats, avian conservation, bird collisions, bird migration, bird mortality, collision risk, migratory birds.

CLASS II. RESEARCH ORIGIN DESCRIPTORS

A. Overall project description:

1. Identity:

Threatscapes for the aeroconservation of birds

2. Originators:

a. Sergio A. Cabrera-Cruz. Unidad de Servicios Profesionales Altamente Especializados, Instituto de Ecología A. C., Xalapa, Veracruz, Mexico.

b. Emily B. Cohen. University of Maryland Center for Environmental Science, Appalachian Laboratory, Frostburg, Maryland, United States.

c. Scott R. Loss. Department of Natural Resource Ecology and Management, Oklahoma State University, Stillwater, Oklahoma, United States.

d. Jeffrey J. Buler. Department of Entomology and Wildlife Ecology, University of Delaware, Newark, Delaware, United States.

3. Period of study:

The first layers of the individual threat maps were created in 2018. The cumulative threat maps were created in 2023.

4. Objectives

General objective: To create high-resolution maps illustrating the distribution and magnitude of bird collision hazards throughout the contiguous United States.

Specific objective 1 (*individual-threat maps*): To quantitatively map the distribution of potential bird collisions throughout the country due to each of the top six sources of anthropogenic bird mortality (aircraft, buildings, communication towers, power lines, roads, and wind turbines).

Specific objective 2 (*cumulative threat maps*): To quantitatively map the cumulative distribution of potential bird collisions inclusive of the top six sources of anthropogenic bird mortality throughout the country.

5. **Abstract:** See above abstract.

6. **Sources of funding:**

During the course of this work, SACC was supported by CONACYT—COVEICyDET PhD scholarships, a Predoctoral Fellowship at the Smithsonian Migratory Bird Center, and by two University of Delaware Doctoral Fellowships. SRL was supported by Hatch Grant Funds (#OKL-03150) from the US Department of Agriculture National Institute of Food and Agriculture and JJB was supported by U.S. Department of Agriculture NIFA Hatch (DEL-00774). No funding to report for EBC.

B. Specific subproject description

1. Site description

a) Site type:

Contiguous United States (48 adjoining states plus the District of Columbia)

b) Geography:

Minimum and maximum longitude (-124.73277, -66.96927) and latitude (24.95638, 49.37173).

c) Habitat:

All habitats and ecoregions in the contiguous United States.

d) Climate:

All climates in the contiguous United States.

2. **Experimental or sampling design**

a) Design characteristics:

See Research methods below.

b) Data collection period, frequency, etc.:

See Research methods below.

3. **Research methods**

a) **Field/laboratory:**

General overview

We obtained comprehensive public geospatial data with the distribution of six threat types responsible for high bird collision-related mortality throughout the contiguous United States (Loss et al. 2015): aircraft, buildings, communication towers, power lines, roads, and wind turbines.

To create the *individual threat maps*, we followed *two steps*. *First*, we generated risk areas for each individual threat, defined as the two-dimensional spatial footprint over the ground where birds may encounter structures or moving vehicles, or where birds may need to take evasive action in order to avoid colliding with these threats. *Second*, as a measure of the magnitude of their potential impact on birds, we assigned to each risk area the annual bird mortality estimated for each threat type, according to published estimates (Longcore et al. 2012, Loss et al. 2013, 2014b, 2014a, 2014c, Dolbeer and Begier 2019), while also accounting for factors affecting variability of those estimates within threat type. We divided the assigned mortality by the area of the threat's risk area, so that our threat maps represent spatially-explicit estimates of potential impact for each threat type. However, these individual threat maps are not meant to represent estimates of expected mortality in any given location, but rather a broad-scale representation of the level of collision threat potentially faced by birds throughout the country.

With this general method, we created 285 state-wide individual-threat maps in raster format with a 30 meter resolution, one for each individual threat type present in each of the 48 contiguous states in the United States, and for the District of Columbia.

To create the *cumulative-threat maps*, we summed each state's individual-threat maps to create state-wide bird-collision threatscapes, representing the cumulative threat level across all threats combined, exclusive of any potential synergistic effects. Thus, the second collection contains 49 spatial rasters displaying the cumulative aerial threat present in each state. In the following paragraphs we provide a detailed description of the methods used to create first the individual-threat maps, and then the cumulative-threat maps.

Individual threat maps

Aircraft

Bird-aircraft collisions (bird strikes) have occurred since the very first flights by the Wright brothers, which resulted in the death of a gull, and they continue to this day (Sodhi 2002, Soldatini et al. 2010, McKee et al. 2016, Metz et al. 2020). Over 305,000 bird strikes with United States-registered civil aircraft have been recorded between 1990 and 2024, with the number of strikes increasing yearly but varying by phase of aircraft flight and airport type (Dolbeer et al. 2025).

In the United States, airports for civilian aviation are broadly classified in two types: those that serve scheduled passenger service (or commercial airports; hereafter part-139 airports, FAA 2023a) and those that do not have scheduled service or have fewer than 2,500 annual passenger boardings (hereafter general aviation airports, FAA 2023a). Most bird strikes at part-139 and general aviation airports in the United States occur at the runway during taxi or during landing rolls, decreasing exponentially with altitude (Dolbeer 2006). The great majority (99%) of bird strikes around part-139 and general aviation airports occur under 3200m agl and 1981m agl (meters above ground level), respectively (Dolbeer and Begier 2019). Hereafter we refer to these altitudes, where 99% of bird strikes cumulatively occur, as the maximum mortality altitudes.

Step 1: Risk areas

Because bird strikes with aircraft occur both in the air and on the ground, we created risk areas that consider both the aerial and terrestrial habitats. To do this, we used as a base the line geometries of runways in all airports in the country (USDOT BTS 2023). We only kept data from civilian airport facilities (i.e. excluding heliports, ballonports, and others, and we did not consider military airports) within the contiguous United States. Furthermore, we only considered airports reported as operational in the Airport Data and Information Portal (FAA 2023b).

We first created ground-level risk areas through rectangular buffers with dimensions equal to the width and length of each runway, representing risk of bird strikes when aircraft are moving before taking off or touching down (Fig. 1). Then, we created aerial risk areas, representing the risk of bird strikes with aircraft in the air, considering multiple factors. The airport environment (i.e. the area under the influence of an airport's operations), where most bird strikes occur, includes the airspace surrounding the airport within the distance needed for aircraft to descend from or to reach maximum mortality altitudes. While aircraft entry flights in preparation for landing may intersect the runway before the actual descent flight (FAA and USDOT 2016), we conservatively assumed that aircraft reach maximum mortality altitudes or descend from them following straight paths (e.g. see Walter et al. 2012). Furthermore, runways can be used in both directions depending on weather patterns at the time of take-off or landing (FAA and USDOT 2016), and we assumed that aircraft at maximum mortality altitudes might be misaligned by up to 10° relative to the runway from which it departed or on which it is preparing to land. Thus, for each airport we created two aerial risk areas shaped like elongated trapezoids, with their short bases connecting with each of the short sides of the terrestrial risk areas, and with outer ends fanning out 10° from the runway, with lengths equal to the distance needed for aircraft to reach or descend from maximum mortality altitudes. In this way, risk areas for bird strikes are associated with airport runways and are hourglass-shaped, with the waist of the hourglass having the width and length of the runway, representing the area where ground-level bird strikes occur, and the containers being two trapezoids where bird strikes in the air may occur (Fig. 1).

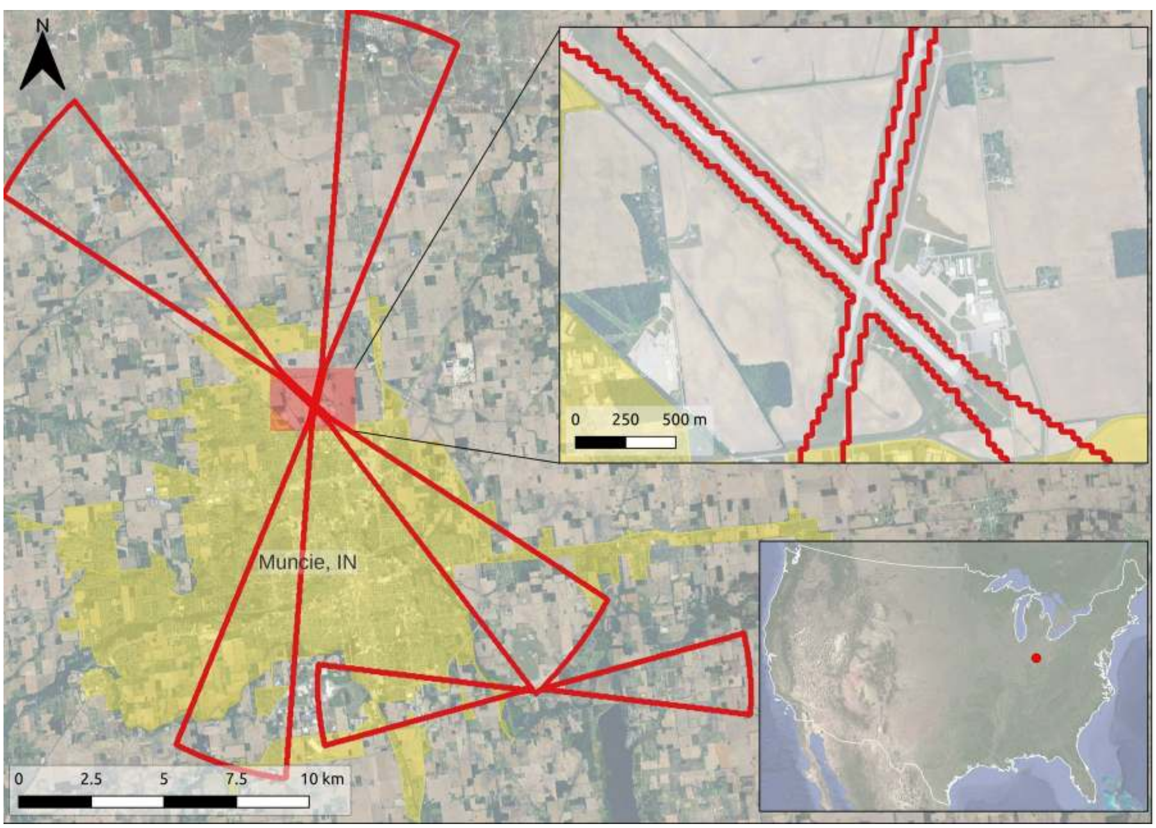

Figure 1. Example of hour-glass shaped risk areas (red polygons) for the bird-aircraft collision threat (bird strikes) associated with runways of the Delaware county regional airport (top) and the Reese airport (bottom) in Muncie, Indiana (semi-transparent yellow polygon). *Top-right:* zoomed-in view to the runways of the Delaware county regional airport. *Bottom-right:* location of Muncie in the United States.

Step 2: Magnitude of impact

For every risk area, we estimated the expected annual bird mortality from bird strikes, considering the expected number of bird strikes by altitude above the ground (Dolbeer and Begier 2019) and the amount of airline traffic according to the airport type (FAA 2023c). To achieve this, we also considered the expected altitude of aicraft in relation to its distance to the runway and up to the maximum mortality altitudes by airport type. The resulting estimates were used as measures of the potential magnitude of impact of the bird-collision with aircraft threat.

To estimate an approximate number of annual bird collisions by height and airport type (Table 1), we first divided the total bird strikes documented between 1990 and 2017 (by height category) by the total number of airports in existence in 2017 (Dolbeer and Begier 2019); then, we divided this by the total number of years (n = 28).

Table 1. Total number of bird collisions with aircraft by height category in feet and by airport type, from Dolbeer and Begier (2019). We estimated the number of "Bird collisions by airport" and height category by dividing the "Total bird collisions" column by 520 (part-139 airports) and by 2009 (general aviation airports) (Table 8 in Dolbeer and Begier, 2019). We then divided this column by 28 (number of years between 1990–2017, all years included), to estimate the number of Bird collisions / airport / year.

Upper limit of bird collision height category		**Part-139 airports (commercial)**			**General aviation airports (non-commercial)**		
Feet (original)	**Meters (rounded)**	**Total bird collisions**	**Collisions / airport**	**Collisions / airport / year**	**Total bird collisions**	**Collisions / airport**	**Collisions / airport / year**
0	0	37256	71.65	2.56	6203	4.17	0.149
500	152	27251	52.41	1.87	6087	4.09	0.146
1500	457	9847	18.94	0.68	2531	1.70	0.061

2500	762	5181	9.96	0.36	1029	0.69	0.025
3500	1067	3784	7.28	0.26	480	0.32	0.012
4500	1372	2256	4.34	0.15	243	0.16	0.006
5500	1676	1615	3.11	0.11	117	0.08	0.003
6500	1981	1064	2.05	0.07	74	0.05	0.002
7500	2286	736	1.42	0.05	58	0.04	0.0014
8500	2591	546	1.05	0.04	34	0.02	0.0008
9500	2895	289	0.56	0.02	20	0.013	0.0005
10500	3200	387	0.74	0.03	20	0.013	0.0005
11500	3505	200	0.38	0.01	4	0.003	0.0001

Then, for each airport type, we fitted a polynomial curve to closely match the observed distribution of bird strikes with aircraft by altitude above ground level (Fig. 2).

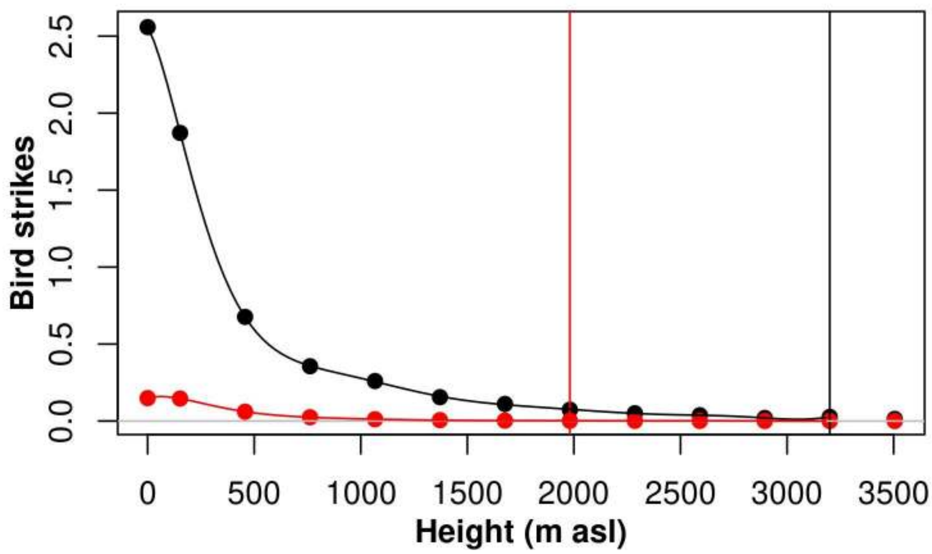

Figure 2. Observed (points) and estimated (lines) annual bird strikes with aircraft for different altitudes at part-139 (black) and general aviation (red) airports in the contiguous United States between 1990 and 2017. Black and red vertical likes represent maximum mortality altitudes (altitude above ground level where 99% of bird strikes cumulatively occur) at part 139 and general aviation airports, respectively. Curves fit observed data with $r^2 > 0.9999$.

We created 30-m rasters with the shape of airport risk areas, with pixels representing aircraft altitudes above the ground, from zero at the runways and up to maximum mortality altitudes. We estimated the expected flight altitude of aircraft assuming that planes ascend and/or descend at constant angles (Fig. 3), and we calculated the ground distance needed for an aircraft to reach maximum mortality altitudes from the ground with the trigonometric function for tangent:

$$\tan(\alpha) = opposite / adjacent$$

or:

$$\tan(Angleofascent) = Mortality\,altitudes / Distance$$

solving:

$$Distance = Mortality\,altitudes / \tan(Anglesofascent)$$

Where:

- Angle of ascent = 15° and 6° for part 139 and GA airports respectively (https://aviation.stackexchange.com/a/22312).
- Maximum mortality altitudes (where 99% of bird strikes cumulatively occur) = 3200m agl and 1981m agl for part-139 and GA airports respectively (Dolbeer and Begier 2019).

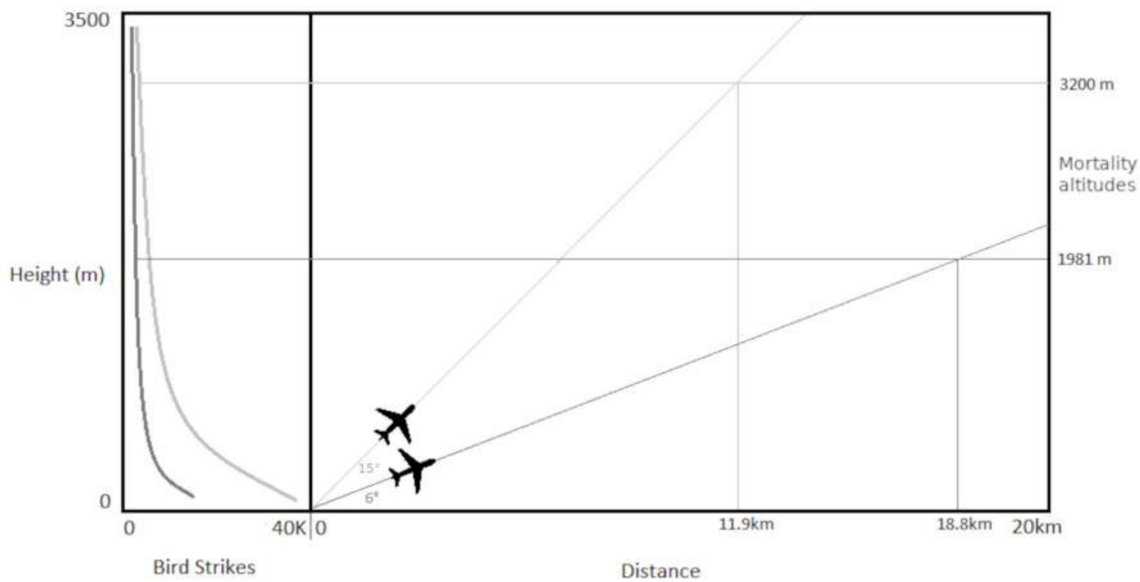

Figure 3. *Left:* Representation of bird strikes by altitude above ground level reported at part-139 (light-gray) and general aviation (dark-gray) airports between 1990 and 2017 in the contiguous United States. *Right:* Distance at which aircraft departing from part-139 and general aviation airports reach maximum mortality altitudes (altitude above ground level where 99% of bird strikes cumulatively occur) after climbing with assumed 15° and 6° constant ascent angles respectively.

We applied the polynomial curve described above to the rasters representing the expected altitude of aircraft at each airport risk area, to estimate their height-based expected number of bird strikes. Then, to obtain an area-based estimate of potential impact of the threat, we divided mortality assigned to each pixel by the by pixel area.

Additionally, we assumed that the risk of bird strikes varies with airport activity, so that the busiest airports represent a higher threat to birds. Thus, we weighted the estimated number of bird strikes by the yearly number of aircraft operations of each airport (FAA 2023b). To do this, we first scaled the number of operations of each airport between zero and 1; we then multiplied the annual expected bird mortality at each airport by their respective scaled number of operations. Because we had already filtered out non-operational airports, we assigned to airports that received a relative risk of zero (i.e. those with zero operations) the second non-zero relative risk, assuming that those airports did have operations but failed to report them to the FAA.

Finally, to create state-wide individual-threat maps quantifying the potential impact of the bird-aircraft collision threat (bird strikes), we mosaicked airports within each state (e.g. Fig. 4).

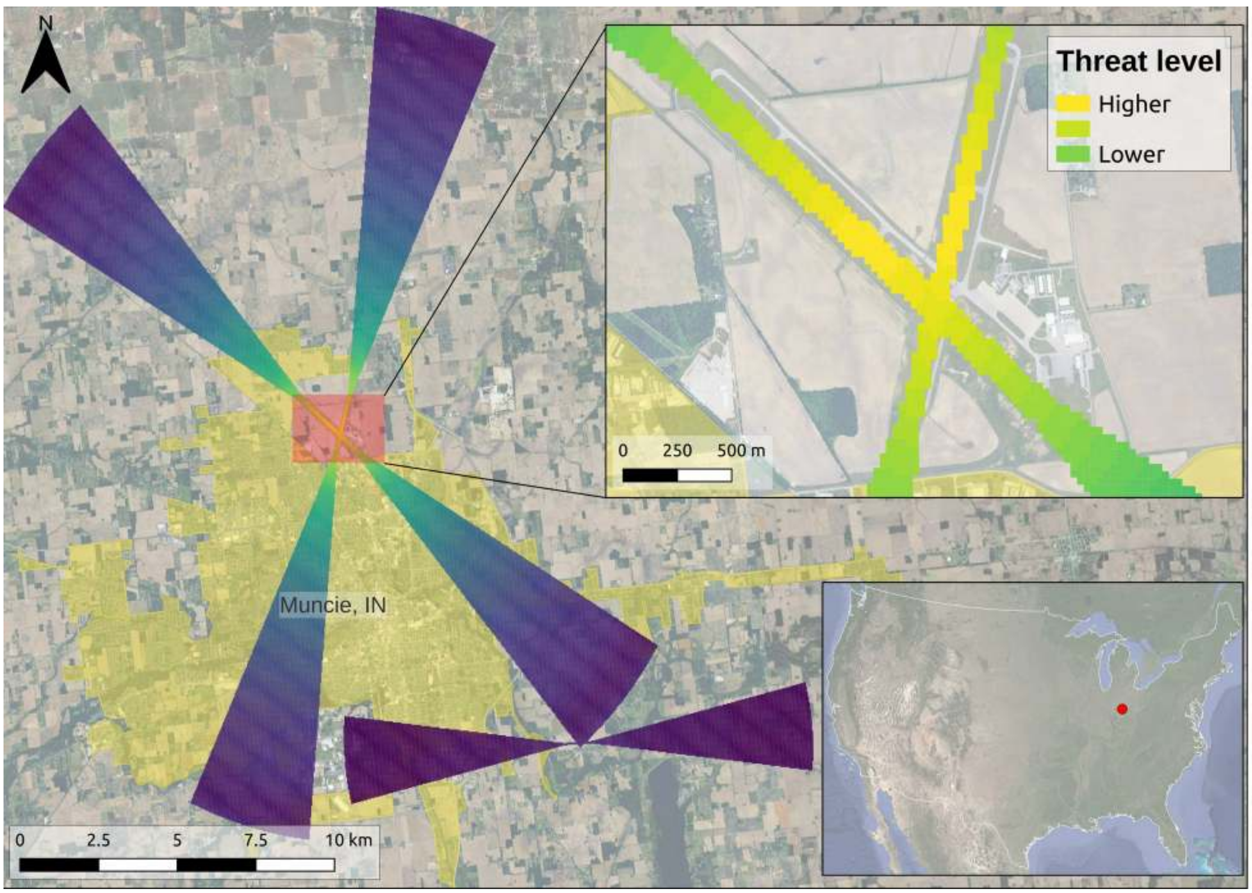

Figure 4. Cumulative-threat map quantifying the potential impact of the bird-aircraft collision threat (bird strikes) for the Delaware county regional airport (top) and the Reese airport (bottom) in Muncie, Indiana (semi-transparent yellow polygon). *Top-right:* zoomed-in view to the runways of the Delaware county regional airport. *Bottom-right:* location of Muncie in the United States.

<u>Buildings (windows)</u>

The transparent and reflective qualities of glass make windows a threat that is hard for birds to detect; hence, bird-window collisions may occur because birds attempt to fly through glass in order to reach vegetation on the other side, or they are deceived by the reflection of vegetation and the sky (Klem 1989, 2025). Reports of window-caused fatalities extend to as early as 1832 (cit. by Klem 2025); nowadays, this threat represents an estimated annual mortality of 365 to 988 million birds in the United States (Loss et al. 2014a), representing the top cause of bird collision-related mortality in the country (Loss et al. 2015).

Step 1: Risk areas

Because bird-window collisions occur at building facades, we defined risk areas as the spatial footprints of buildings (Fig. 5). We obtained existing building footprints for the contiguous United States, by downloading the USBuildingFootprints datasets for all 48 contiguous states and the District of Columbia (Microsoft 2018).

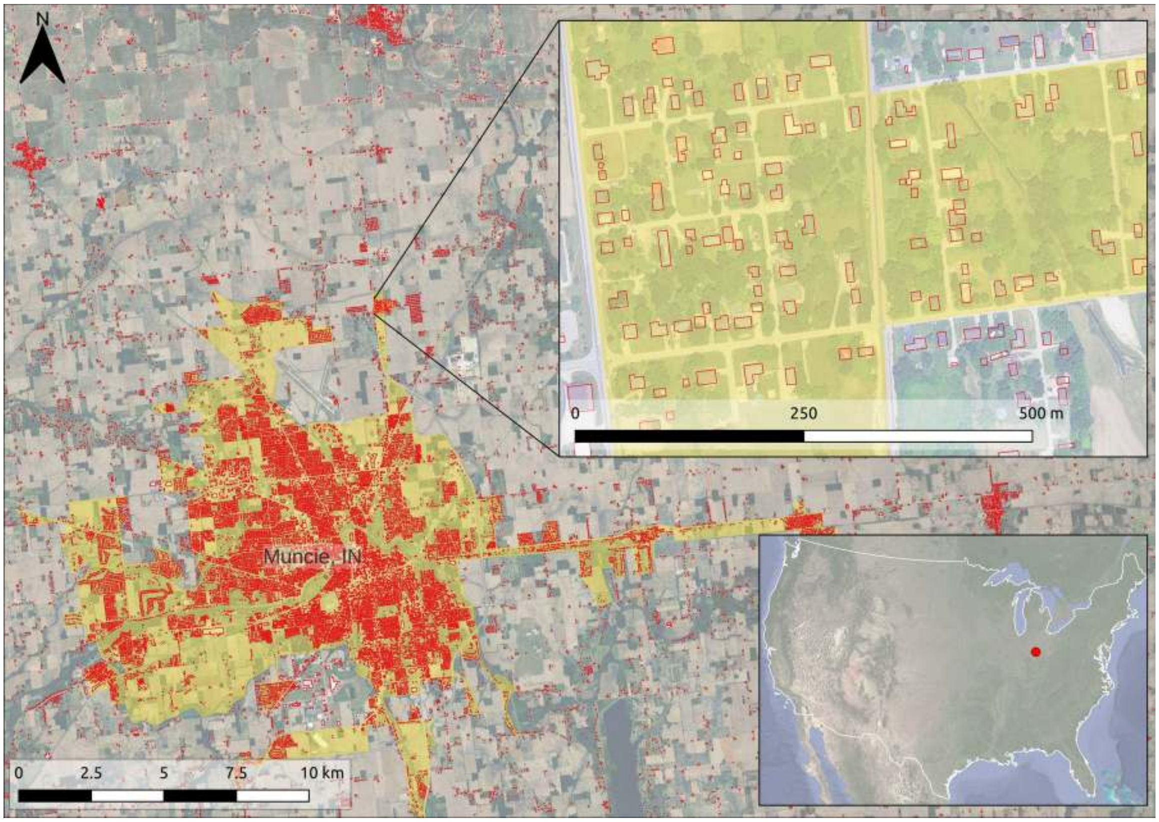

Figure 5. Building footprints (red polygons) in and around Muncie, Indiana (semi-transparent yellow polygon). *Top-right:* zoomed-in view to buildings in a neighborhood north of Muncie . *Bottom-right:* location of Muncie in the United States.

Step 2: Magnitude of impact

Not all buildings pose the same level of threat to bird collisions. The estimated number of birds killed annually by collisions with windows varies by building height (Loss et al. 2014a), and by the interaction between building size and regional urbanization, such that the greatest collision-related mortality occurs at large buildings in areas with low levels of surrounding urbanization (Hager et al. 2017, Elmore et al. 2021).

To incorporate the variable estimates of bird-window collisions in relation to building height, we first assigned to each building footprint an approximate height, taken from the US map of estimated building heights by block (Falcone 2016). Then, we assigned to each building footprint the estimated number of bird fatalities/year according to its height, matching as closely as possible the height categories in Loss et al. (2014a; **Table 2**).

Table 2. Annual bird mortality per building by building height categories, and building heights by block assigned to building footprints.

Bird mortality estimates (Loss et al. 2014)		**Building heights by block group (Falcone 2016)**	
Annual bird mortality / building	**Aggregate height categories**	**Category**	**Description**
2.1	Residences (1–3 stories)	Low	Lowest category of building heights; primarily 1-2 story buildings
		Low-medium	2nd lowest category; primarily 2-3 story buildings
27.1[a]	Low-rise (4 – 11 stories)	Medium	3rd lowest category; primarily 3-4 story buildings
		Medium-High	3rd highest category; primarily 3-6 story buildings
		High	2nd highest category: primarily 4-9 story buildings
24.3	High rise (≥12 stories)	Very-High	Highest category of building heights; buildings average 10 stories or higher

[a] Estimate based on year-round studies of bird-building collisions (Loss *et al.* 2014) .

To further incorporate the effect of regional urbanization on bird-window collision mortality estimates, we used the 2019 National Land Cover Database (NLCD; Homer et al. 2012). The NLCD identifies 20 different land cover types across the United States with a 30 m resolution, including four levels of developed lands with varying degrees of development intensity. All levels of development in the NLCD are defined as having some degree of constructed materials and impervious surfaces (https://www.mrlc.gov/data/legends/national-land-cover-database-class-legend-and-description). We reclassified the NLCD, assigning values 1– 4 to each of the four categories of developed land cover types with increasing intensity (**Table 3**). Furthermore, considering that modified landscapes extend beyond urban to rural gradients (Ellis and Ramankutty 2008), and that the NLCD might miss single buildings outside this gradient given its spatial resolution, we assigned a value of 0.1 to all other land cover classes to represent very low development. We then estimated the maximum value of land cover development within each building footprint.

Table 3. Reclassified values from the original NLCD classification, used to estimate urban development within building footprints.

NLCD land cover classification		**Reclassified values**
Code	**Code name**	
24	Developed, high intensity	4 (High)
23	Developed, medium intensity	3 (Medium)
22	Developed, low intensity	2 (Low)
21	Developed, open space	1 (Low)
1 – 20 and >24	See NLCD legend*	0.1 (Very low)

* Available at https://www.mrlc.gov/data/legends/national-land-cover-database-2019-nlcd2019-legend

The effect of regional urbanization on bird-window collisions is most noticeable for large buildings (Hager et al. 2017). For example, the average number of bird carcasses/day expected for medium and small buildings is almost the same regardless of regional urbanization around the buildings (Hager *et al.* 2017). For large buildings, however, the number of carcasses expected at low-urbanization areas is nearly twice the number expected for large buildings surrounded by average levels of urbanization (Hager *et al.* 2017). On the other hand, the number of carcasses expected at large buildings in highly-urbanized areas is almost half as in average-urbanized areas (Hager *et al.* 2017). We assumed that the estimated annual bird mortality per building in Loss *et al.* (2014a) corresponds with the number of carcasses/day estimated for average urbanization levels in Hager et al. (2017). Thus, we weighted annual bird mortality for large buildings by level of urbanization. To do this, we doubled or halved mortality estimates/building for high-rise buildings, depending on the estimated urban development from our reclassified NLCD, leaving unchanged the mortality estimates for residences and low-rise buildings.

Finally, to create state-wide individual-threat maps quantifying the potential impact of the bird-window collision threat, we rasterized risk areas with a 30 m resolution, first dividing the mortality assigned to each risk area by the area of their own spatial footprint, thus obtaining an area-based estimate of potential impact of the bird-window collision threat (e.g. Fig. 6).

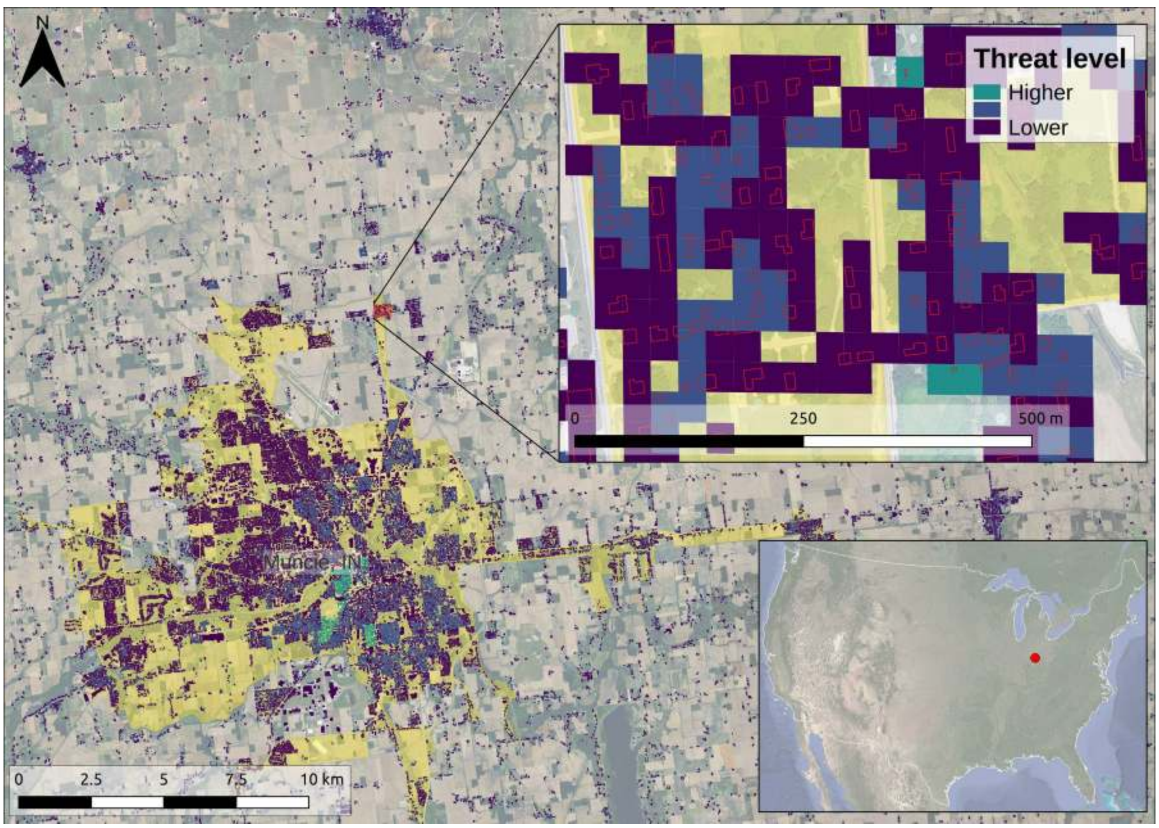

Figure 6. Cumulative-threat map quantifying the potential impact of the bird-window collision threat in Muncie, Indiana (semi-transparent yellow polygon). *Top-right:* zoomed-in view to buildings in a neighborhood north of Muncie. *Bottom-right:* location of Muncie in the United States.

Communication towers

The earliest published study on bird mortality due to collisions with communication towers dates back at least to1949 (Gehring et al. 2009). Collisions with communication towers ≥60 m tall cause approximately 6.6 million bird fatalities in the continental United States, with the number of annual fatalities varying by tower altitude and tower characteristics (e.g. towers with strobe lights vs. steady-burning lights; Longcore et al. 2012).

Step 1: Risk areas

To create bird collision risk areas around communication towers, we used geospatial data with the distribution of tall structures that represent an obstacle for aircraft. The digital obstacle file (DOF) is a data set compiled by the Federal Aviation Administration of the United States that describes known obstacles to aviation in North America, the Caribbean and the Pacific, including communication towers. The DOF lists structures taller than 200ft (~61m) above ground level, as well as lower structures near airports (see https://www.faa.gov/air_traffic/flight_info/aeronav/obst_data/doffaqs/), identifying them by type (see full list of obstacle types https://www.faa.gov/air_traffic/flight_info/aeronav/obst_data/structuretypes/) and providing their location (coordinates) and height, as well as estimates of accuracy for the location and height of all obstacles. Furthermore, the DOF also indicates whether the presence of each structure has been verified, and if it is still present or has been dismantled.

We downloaded the 05 September 2021 version of the DOF (latest version available at https://www.faa.gov/air_traffic/flight_info/aeronav/digital_products/dof/), and kept for further processing only standing towers taller than 60m within the contiguous United States that had been verified and had height and location accuracy of ±15.2 m (50 ft) and ±76.2 m (250 ft) respectively. We then created risk areas around each tower representing the maximum distance needed by a hypothetical nocturnally migrating bird to avoid collision with a tower. This risk area was defined as a circle around each tower with radius equal to the distance needed by a nocturnally migrating bird to fly over the tower after taking off from the ground (Fig. 7), if ascending at a constant angle of 11.8°—the average of climb angles in Table 2 of Able (1977) and heading straight towards the tower without changing direction.

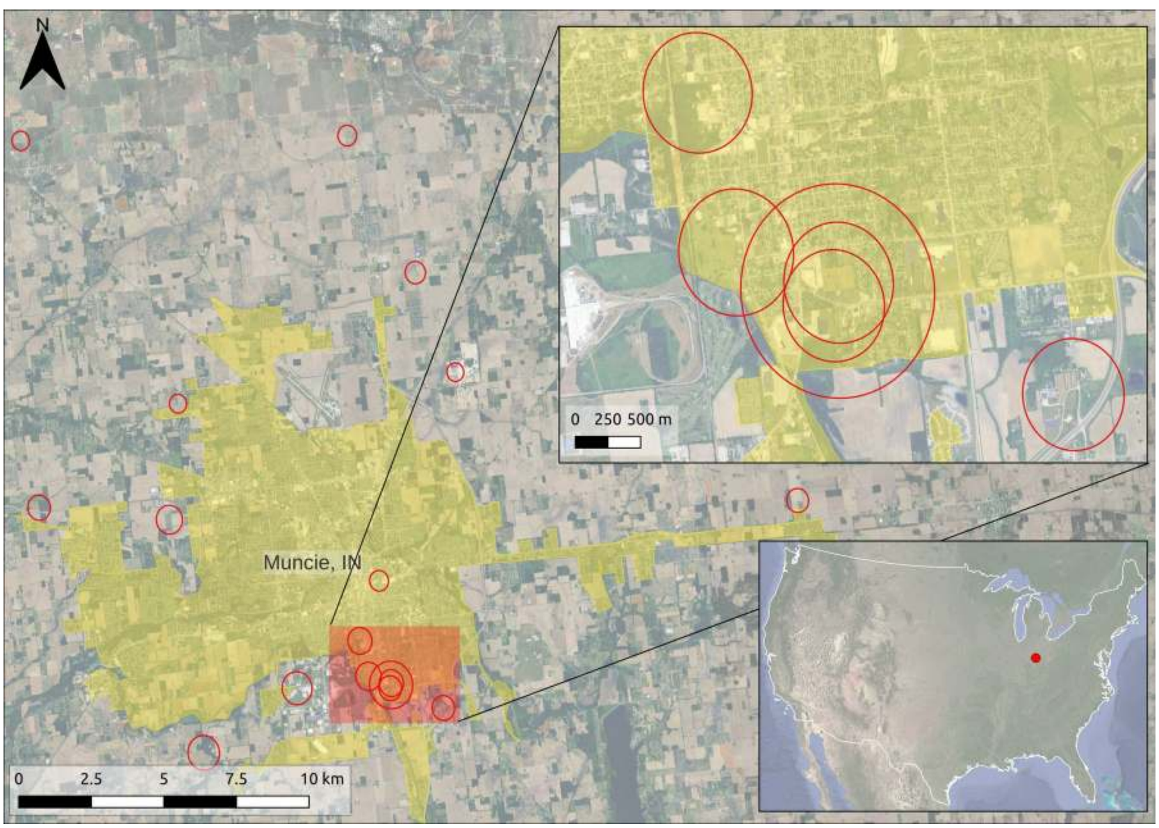

Figure 7. Example of circular risk areas (red polygons) associated to communication towers in and around Muncie, Indiana (semi-transparent yellow polygon). *Top-right:* zoomed-in view to risk areas south of Muncie. *Bottom-right:* location of Muncie in the United States.

Step 2: Magnitude of impact

For every risk area, we estimated the expected number of annual bird collisions considering the height of communication towers. To do this, we first divided the total number of annual fatalities reported in Table 7 of Longcore et al. (2012) by the sum of all towers within that category. We then assigned the estimated annual mortality/tower to each risk area according to tower height.

Finally, to create state-wide individual-threat maps quantifying the potential impact of the bird-communication tower-collision threat, we rasterized risk areas around towers with a 30 m resolution, first dividing the mortality assigned to each risk area by the area of their own spatial footprint, thus obtaining an area-based estimate of potential impact of the bird-communication tower collision threat (e.g. Fig. 8).

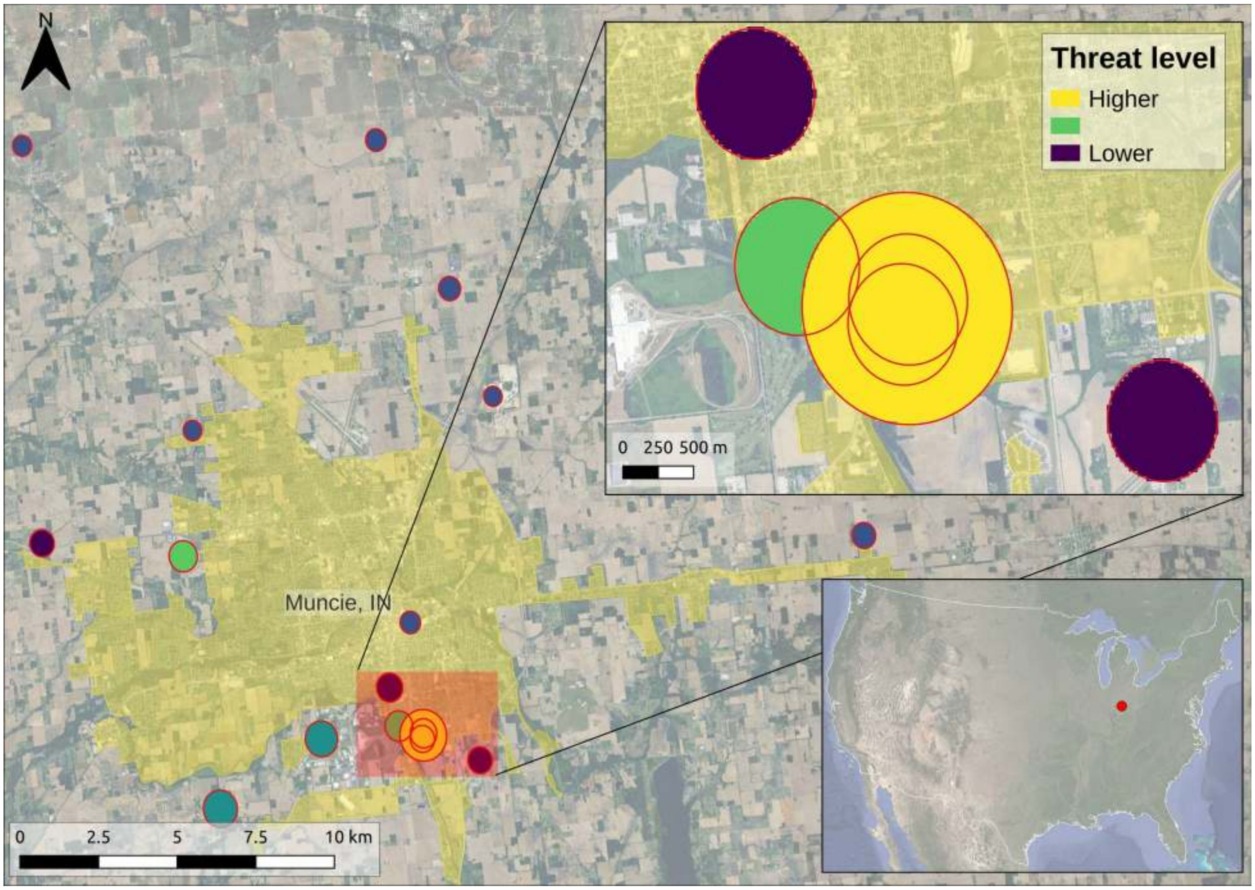

Figure 8. Cumulative-threat map quantifying the potential impact of the bird-communication tower collision threat in and around Muncie, Indiana (semi-transparent yellow polygon). *Top-right:* zoomed-in view to risk areas south of Muncie. *Bottom-right:* location of Muncie in the United States.

Power lines

Overhead cables represent a difficult-to-detect threat for birds (Martin and Shaw 2010) that has caused bird collisions fatalities since the nineteenth century (Coues 1876, Emerson 1904). Overhead power lines can be categorized in two types: transmission lines and distribution lines, the former carrying high voltages (>60 kV) from power plants and the latter carrying and delivering lower voltage electricity (<60 kV) to end consumers (Bernardino et al. 2018). In the continental United States, between 8 and 57 million birds are killed annually by collision with overhead power lines (Loss et al. 2014c).

Step 1: Risk areas

To create bird collision risk areas around overhead power lines in the continental United States, on October 15 2021 we downloaded the United States Electric power transmission lines geospatial dataset from the Homeland Infrastructure Foundation-Level Data (HIFLD; downloaded from https://hifld-geoplatform.opendata.arcgis.com/datasets/electric-power-transmission-lines/about, but link not working when last checked on May 18 2026. Current access to this dataset appears to be available at https://www.dhs.gov/gmo/gii, but user credentials are needed).

The downloaded dataset indicates whether the power line is overhead or underground, and whether it is in service or has been removed. We kept all overhead power lines (n = 88601*)* as well as those with no details (n = 683) within the contiguous United States marked as "in service" and "inactive", and removed those marked as proposed and under construction (n = 25). In order to preserve the geographical coverage of the data, we also included power lines with status "not available", because these represented 20.1% of all overhead power lines in the dataset and were concentrated in the western United States.

We created risk areas by adding 25m-wide buffers around all power lines (Fig. 9), with buffer length defined by the average reaction distance of flying Passerine birds to transmission lines (Ventana Wildlife Society 2009).

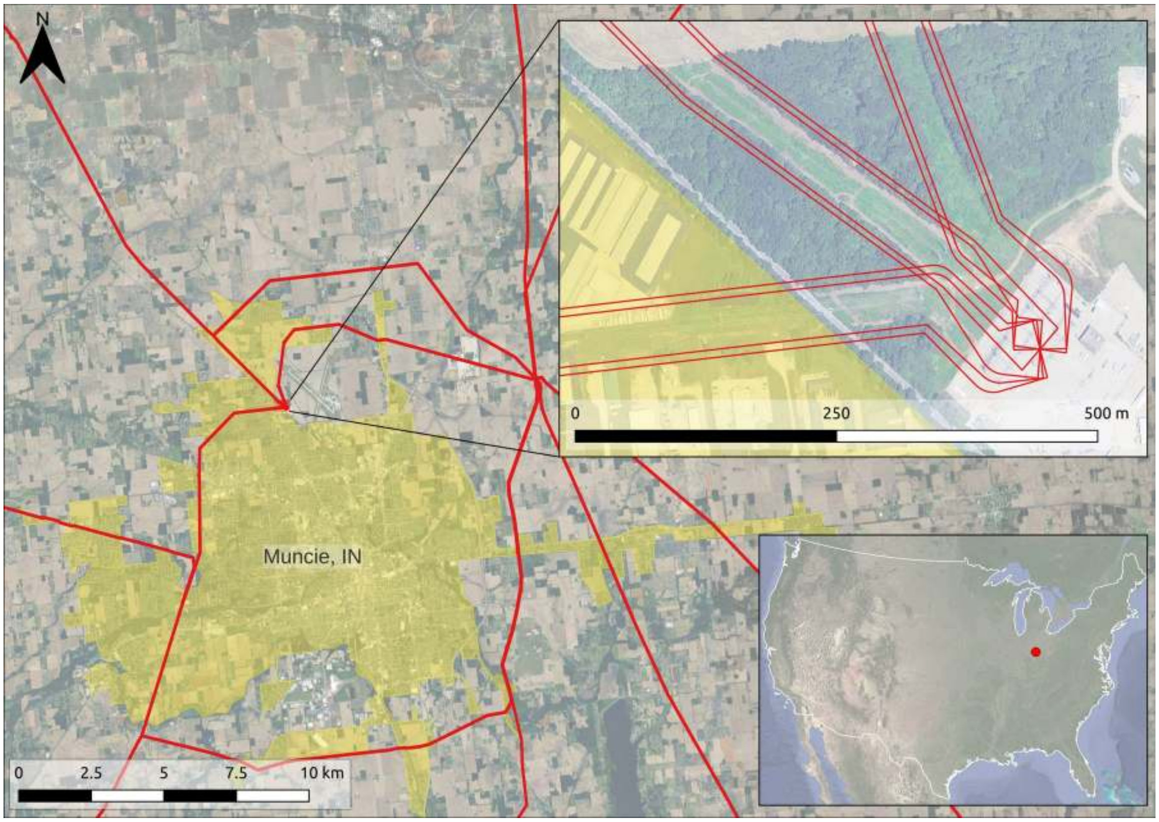

Figure 9. Example risk areas (red polygons) for the bird-power line collision threat associated with overhead power lines in and around Muncie, Indiana (semi-transparent yellow polygon). *Top-right*: zoomed-in view to a substation north of Muncie where a set of power lines originate. *Bottom-right*: location of Muncie in the United States.

Step 2: Magnitude of impact

For every risk area, we estimated the expected number of annual bird collisions considering the type of power lines (transmission or distribution). The downloaded dataset also indicates the voltage transmitted by power lines (range = 3–1000 kV). We categorized power lines with stated voltages ≤60 kV as distribution lines and those with voltages >60 kV as transmission lines (APLIC 2012). Nearly 17% of power lines in the dataset did not report voltage, so we conservatively considered them distribution lines (i.e. transmitting low voltage) because these are responsible for a lower number of bird fatalities compared to transmission lines (see below).

We estimated the expected bird mortality/km of power line by multiplying the length of each geospatial line feature (i.e. each power line, as represented in the dataset) times the median annual estimate of bird mortality/km of power lines in the United States (Loss et al. 2014c). For transmission lines, we multiplied line length times 29.6, the median estimate of bird mortality/km obtained using the strictest criteria of data inclusion in Loss et al. (2014c); we used this value because the authors reported it as likely producing the least biased mortality estimate. For distribution lines, we multiplied line length times 2.93, the average bird mortality/km of the three studies on bird collision with distribution lines in the United States cited in Table 1 of Loss et al. (2014c).

Finally, to create state-wide individual-threat maps quantifying the potential impact of the bird-power line-collision threat, we rasterized risk areas around power lines with a 30 m resolution, first dividing the mortality assigned to each risk area by the area of their own spatial footprint, thus obtaining an area-based estimate of potential impact of the bird-power line collision threat (e.g. Fig 10).

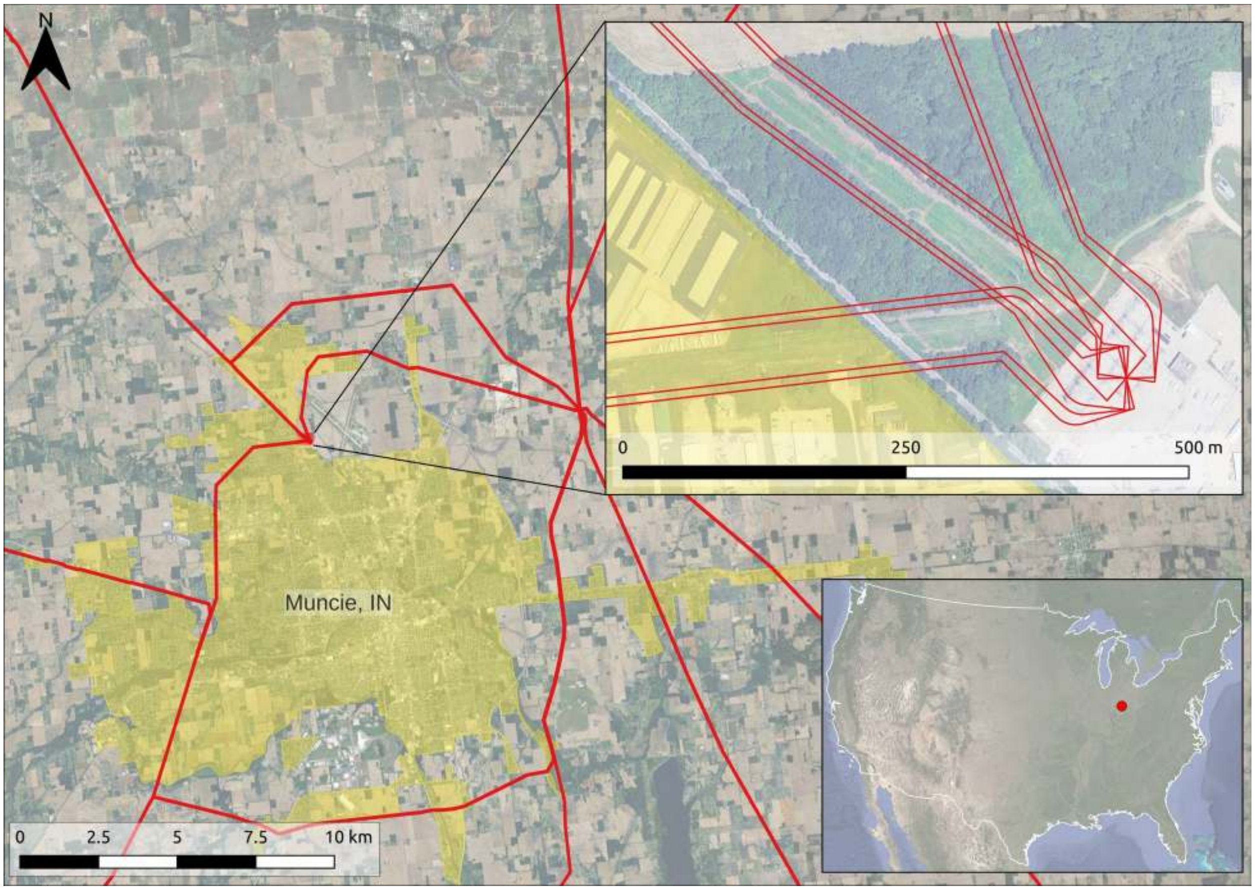

Figure 10. Cumulative-threat map quantifying the potential impact of the bird-power line collision threat associated with overhead power lines in and around Muncie, Indiana (semi-transparent yellow polygon). *Top-right:* zoomed-in view to a substation north of Muncie where a set of power lines originate. *Bottom-right:* location of Muncie in the United States.

Roads

Bird mortality from collisions with automobiles has been documented for nearly a century (Stoner 1925, 1936, Spiker 1927, White 1927), likely from the moment when cars reached speeds that made it impossible for birds to avoid them. Cars in the continental United States move through a road network 4 million miles long (USDT FHA 2014). The extent of this road network and the volume of vehicles circulating through it makes collisions with cars the second most important source of bird collision-related mortality in the continental United States (Loss et al. 2015). This threat is estimated to kill, annually, between 89 and 340 million birds in the country (Loss et al. 2014b).

Step 1: Risk areas

To create bird collision risk areas around roads in the continental United States, we used the Highway Performance Monitoring System (HPMS), the information system for all public roads in the United States (available at https://www.fhwa.dot.gov/policyinformation/hpms.cfm). The HPMS classifies roads in seven types, further grouped into four main categories. First, the interstate system, which provides the highest level of mobility and the highest speeds (55 – 75 mi/h) over the longest uninterrupted distance. Second, two types of major arterials and one type of minor arterial, all of which include important roadways that supplement the interstate system (with speeds in the 50 – 70 mi/h range). Third are the major and minor collectors, which connect local roads and streets with arterials (speeds 35 – 55 mi/h). Fourth are the local roads, which are the primary access to local areas such as residences, businesses and farms at speeds ranging between 20 and 45 mi/h (USDOT FHWA 2000). Roads are also classified in six “facility types”, defined as the operational characteristic of the roadway, including, for example one-way roadways, two-way roadways and ramps.

We downloaded the HPMS with data updated for year 2016 (https://www.bts.gov/ntad), and kept roads within the contiguous United States only. We assumed that roads with the lowest speed limit represent a relatively low risk to birds, so we conservatively deleted all local roads and minor collectors from the database. We also deleted tunnels and roads planned or not built.

We created risk areas around roads by adding 37.5m-wide buffers for all roads (Fig. 11), with buffer length representing the average flight initiation distance of non-raptor birds in response to approaching vehicles (Legagneux and Ducatez 2013).

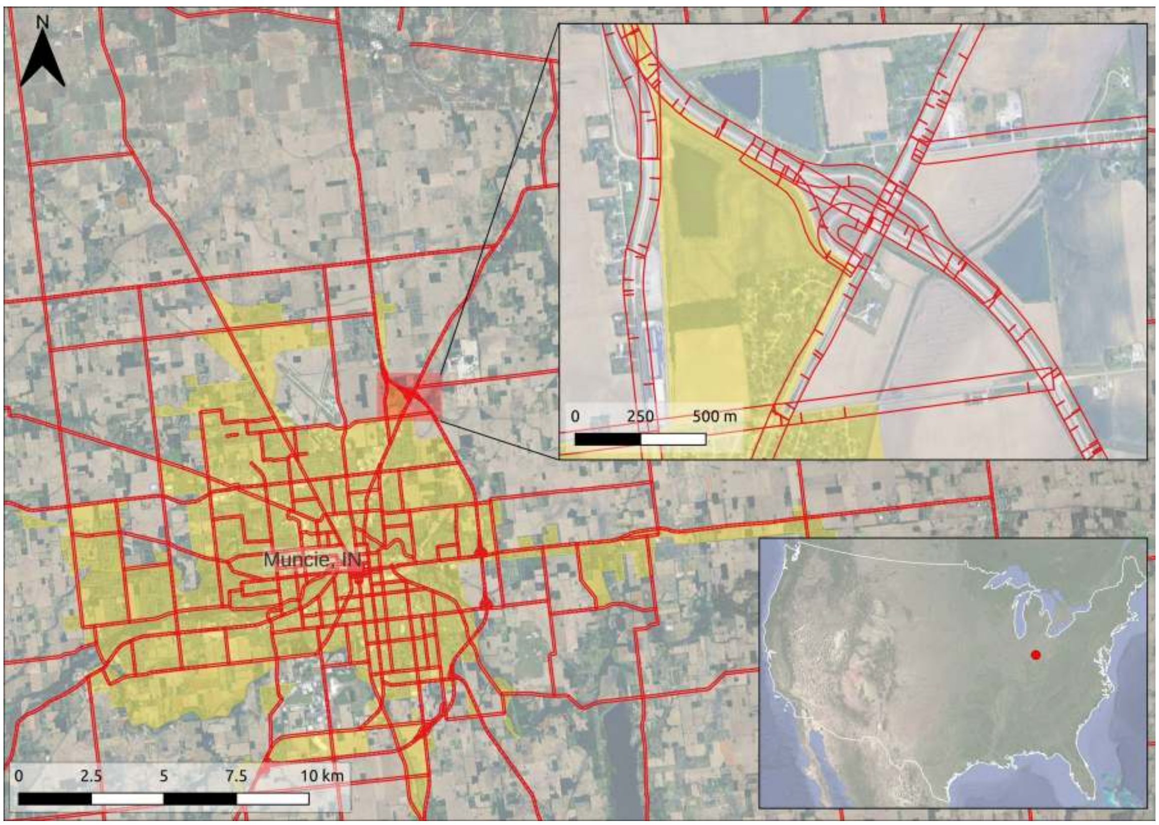

Figure 11. Example risk areas (red polygons) for the bird-car collision threat associated with roads in and around Muncie, Indiana (semi-transparent yellow polygon). *Top-right:* zoomed-in view to roads and an intersection north of Muncie. *Bottom-right:* location of Muncie in the United States.

Step 2: Magnitude of impact

For every risk area, we estimated the expected number of annual bird collisions by road length, considering the road's annual average daily traffic (AADT), an estimate of road traffic intensity available in the HPMS dataset. However, not all roads in the database contain an AADT. To account for this, we estimated the average AADT for each combination of road type and facility type. Thus, for roads without an specified AADT in the HPMS, we assigned the average based on their road type and facility type. For roads that still received an AADT of zero (i.e. there was not an AADT for a given combination of road and facility type), we assigned the lowest non-zero AADT in the database.

Some roads in the database are represented by multiple segments of a contiguous line (*i.e.* a polyline). We aggregated roads by their national identifier number, summing up the AADT of each segment in order to get the total traffic estimate for the entirety of each road. We then scaled the aggregated AADT between zero and 1 to use it as a weighing factor of bird-vehicle collisions based on traffic. We assigned the lowest non-zero value to roads that received a scaled AADT of zero.

We estimated the length of each road in kilometers, and calculated the expected bird mortality for each road by multiplying road length by 36, the annual median bird mortality per kilometer of road in the continental United States (Loss et al. 2014b). We then multiplied this times the scaled AADT, thus weighing potential bird mortality/km by road traffic.

Finally, to create state-wide individual-threat maps quantifying the potential impact of the bird-cars-collision threat, we rasterized risk areas around roads with a 30 m resolution, first dividing the mortality assigned to each risk area by the area of their own spatial footprint, thus obtaining an area-based estimate of potential impact of the bird-car collision threat (Fig. 12).

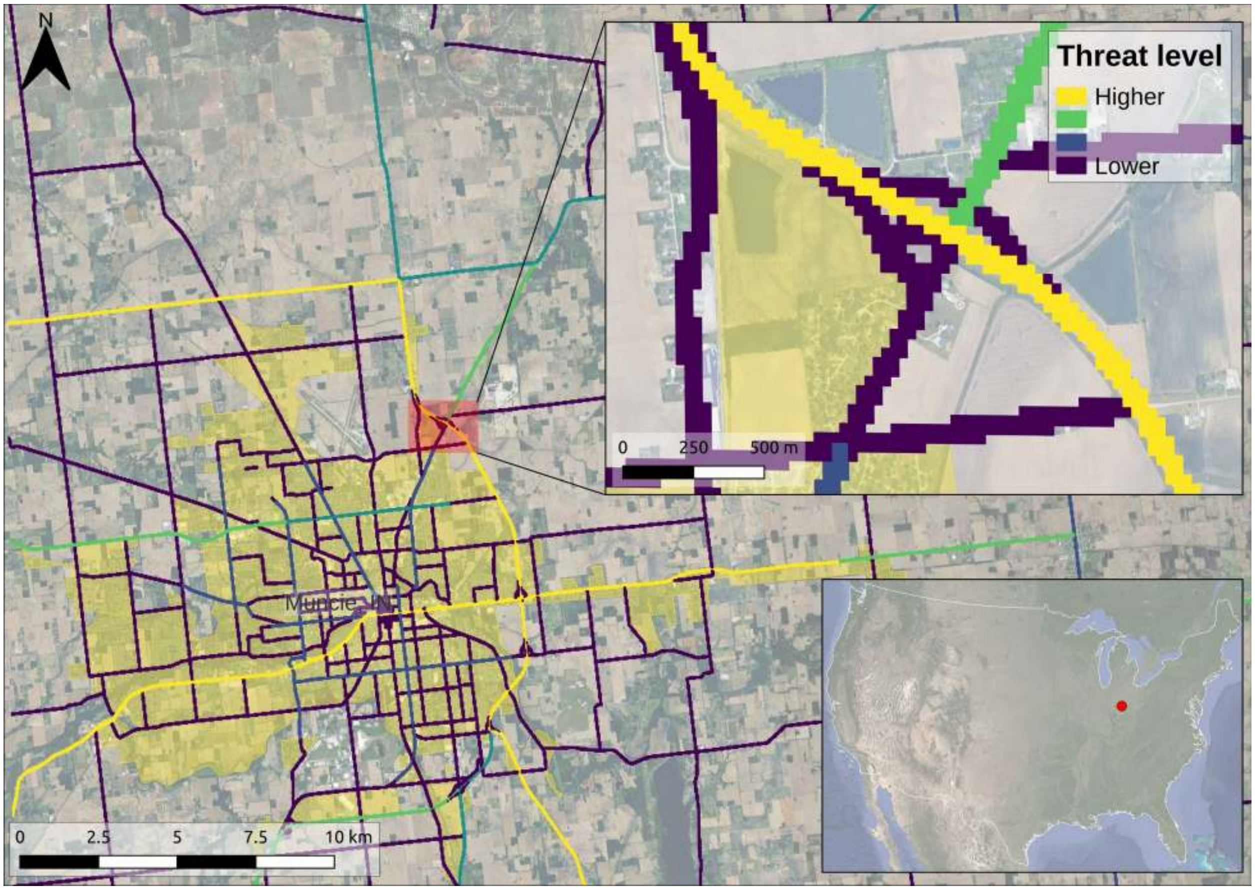

Figure 12. Cumulative-threat map quantifying the potential impact of the bird-car collision threat associated with roads in and around Muncie, Indiana (semi-transparent yellow polygon). *Top-right:* zoomed-in view to roads and an intersection north of Muncie. *Bottom-right:* location of Muncie in the United States.

Wind turbines

Collisions with modern wind turbines in the United States were recorded even before the first large-scale wind farm was built in the country in 1980, when one Starling (*Sturnus vulgaris*) was found dead at the base of the single experimental wind turbine that was being studied to evaluate the potential environmental effects of these structures (Rogers et al. 1977, Kessler 2017, Wind Energy Center 2021). Currently, one highly-cited annual estimate of the average number of bird collisions with wind turbines in the continental United States is 234,000 (range = 140,000 – 328,000), with the expected annual mortality per megawatt of energy generated varying regionally within the country (Loss et al. 2013).

Step 1: Risk areas

To create bird collision risk areas around wind turbines in the continental United States, we used geospatial data from the US wind turbine database (USWTDB). The USWTDB (Hoen et al. 2018) contains the location of wind turbines throughout the country, as well as technical specifications such as turbine height and the turbine rated capacity. We downloaded the USWTDB and removed records outside the contiguous United States, as well as records with low confidence in wind turbine location and attributes (Rand et al. 2020). We further removed 3 turbines from the data set, all from the *Tehachapi Wind Resource Area 1* in Kern county, California, which had no declared turbine height or turbine capacity. We estimated the median height of all wind turbines (126.5 meters) and assigned it to the 768 turbines with no declared height.

We created risk areas around wind turbines similar to those for communication towers: circular areas around each turbine with radius equal to the distance needed by a bird to fly over the turbine's maximum height (Fig. 13), after taking off from the ground and heading straight towards the turbine, without changing direction, while ascending at a constant angle of 11.8 degrees (Able 1977).

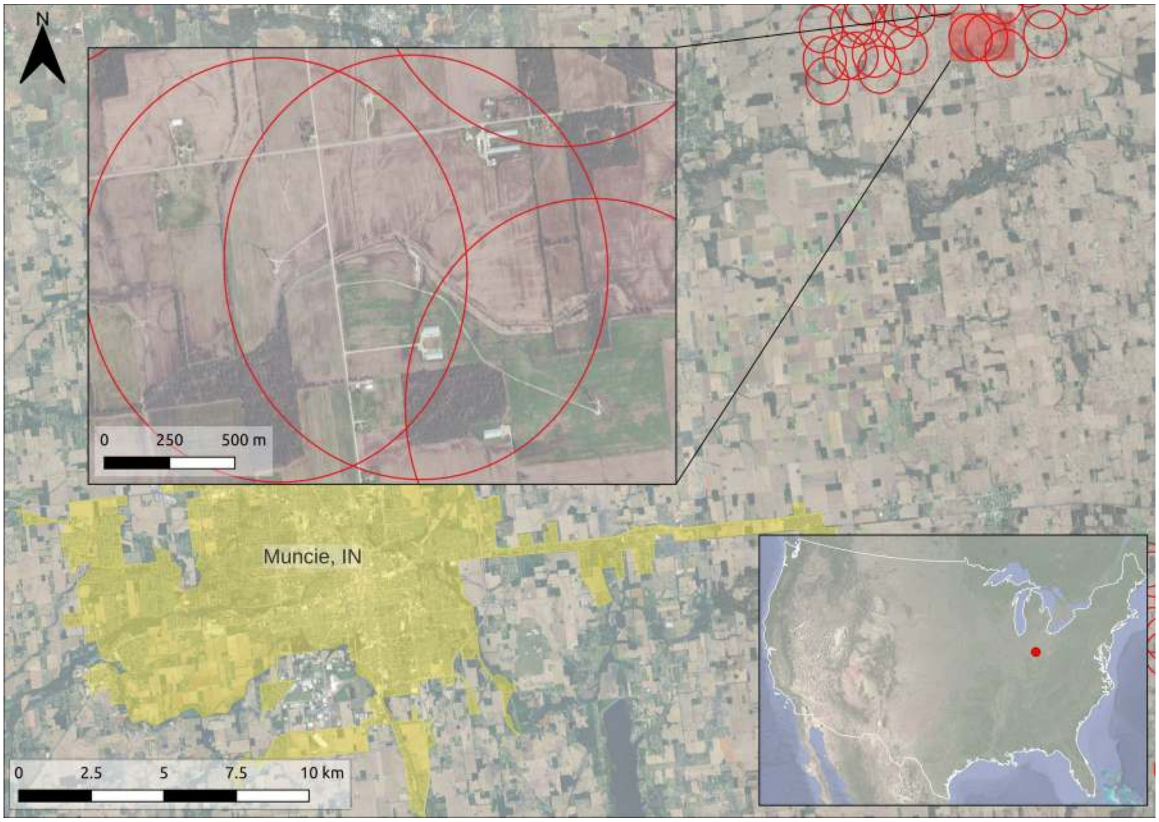

Figure 13. Example of circular risk areas (red polygons) for the bird-wind turbine collision threat associated with wind turbines northeast of Muncie, Indiana (semi-transparent yellow polygon). *Top-left:* zoomed-in view to risk areas. *Bottom-right:* location of Muncie in the United States.

Step 2: Magnitude of impact

For every risk area, we estimated the expected annual mortality per megawatt (bird mortality/MW) at every wind turbine, considering the regional location of turbines. However, the rated capacity of turbines is provided in the USWTDB in kilowatts (kW; see the field definition of 't_cap' https://energy.usgs.gov/uswtdb/api-doc/#keyValue). Hence, we first estimated wind turbine capacity in MW by dividing turbine rated capacity in kW by 1000. Then, we classified wind turbines geographically into the same four broad United States regions defined by Loss et al. (2013). Finally, we multiplied each turbine capacity in MW times the region-specific estimates of bird mortality/MW (Table 4).

Table 4. Four geographic regions in the contiguous United States used by Loss et al. (2013), and regional estimates of bird mortality/MW, by the same authors.

Region	Abbreviation of United States States included	Bird mortality/MW
California	CA	18.76
West	AZ, NV, UT, ID, OR, WA, MT, WY	2.83
Plains	ND, MN, SD, IA, NE, CO, KS, NM, OK, TX	1.81
East	WI, IL, MO, AR, LA, MS, TN, KY, IN, MI, OH, AL, GA, FL, SC, NC, VA, WV, PA, DC, MD, DE, NJ, NY, CT, RI, MA, NH, VT, ME	3.86

Finally, to create state-wide individual-threat maps quantifying the potential impact of the bird-wind turbine collision threat, we rasterized risk areas around wind turbines with a 30 m resolution, first dividing the mortality assigned to each risk area by the area of their own spatial footprint, thus obtaining an area-based estimate of potential impact of the bird-wind turbine collision threat (Fig. 14).

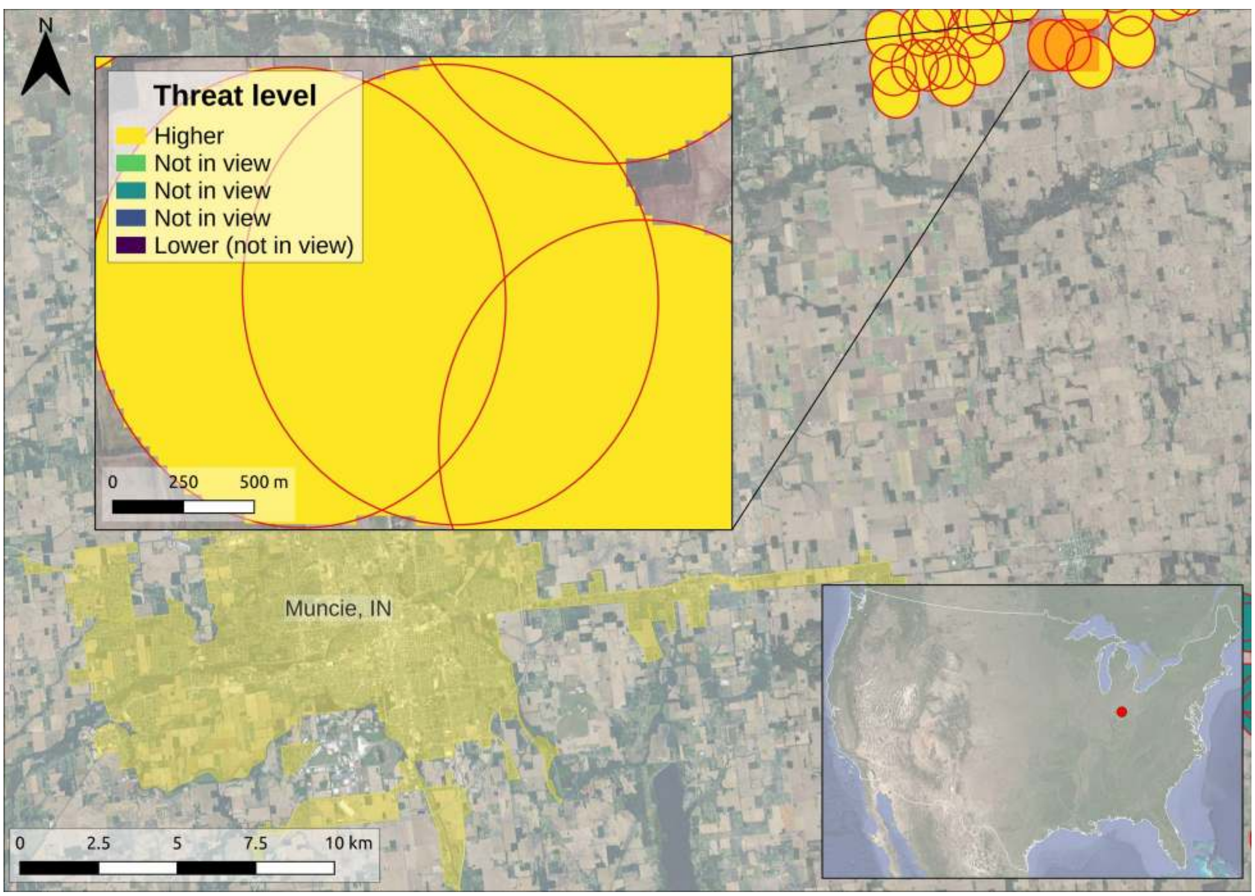

Figure 14. Cumulative-threat map quantifying the potential impact of the bird-wind turbine collision threat for wind turbines northeast of Muncie, Indiana (semi-transparent yellow polygon). *Top-left:* zoomed-in view to risk areas. *Bottom-right:* location of Muncie in the United States.

Rescaling of individual-threat maps

The estimates of annual bird collisions varies by orders of magnitude depending on threat type (Loss et al. 2015). Similarly, the spatial footprint of our risk areas varies from tens (e.g. a single building footprint) to thousands square meters (e.g. risk area associated to an airport runway). Consequently, our area-based estimates of potential bird mortality assigned to risk areas also varied by orders of magnitude, potentially making the comparison between individual-threat maps challenging.

Additionally, while we used bird mortality estimates as a measure of the potential impact that each threat has on birds, our threatscapes are not intended to represent the expected mortality in any given location. Hence, all threat maps should be taken simply as estimates of the potential collective impact of the top six bird-collision threats, and not as actual estimates of expected bird mortality at any given location.

To simultaneously make the values in the individual-threat maps more comparable both among threats and states, and to prevent unintended miss-interpretations of their values, we rescaled the assigned mortality estimates between 0 and 100, with zero representing threat-free pixels and 100 representing pixels with the maximum threat level. The scaling was done considering the overall, country-wide, minimum and maximum threat levels. Considering all states evaluated, the minimum threat level for all threats and states is zero because there are threat-free areas throughout the country, but the maximum threat levels vary by state and threat type.

Cumulative threat maps

To create the state-wide cumulative-threat maps representing the cumulative potential impact of all six bird-collision threats, we summed individual-threat maps of each state (e.g. Fig. 15). Before summing, however, we assigned a value of 0 (zero) to all pixels with no threats present, thus giving a numeric value to threat-free areas.

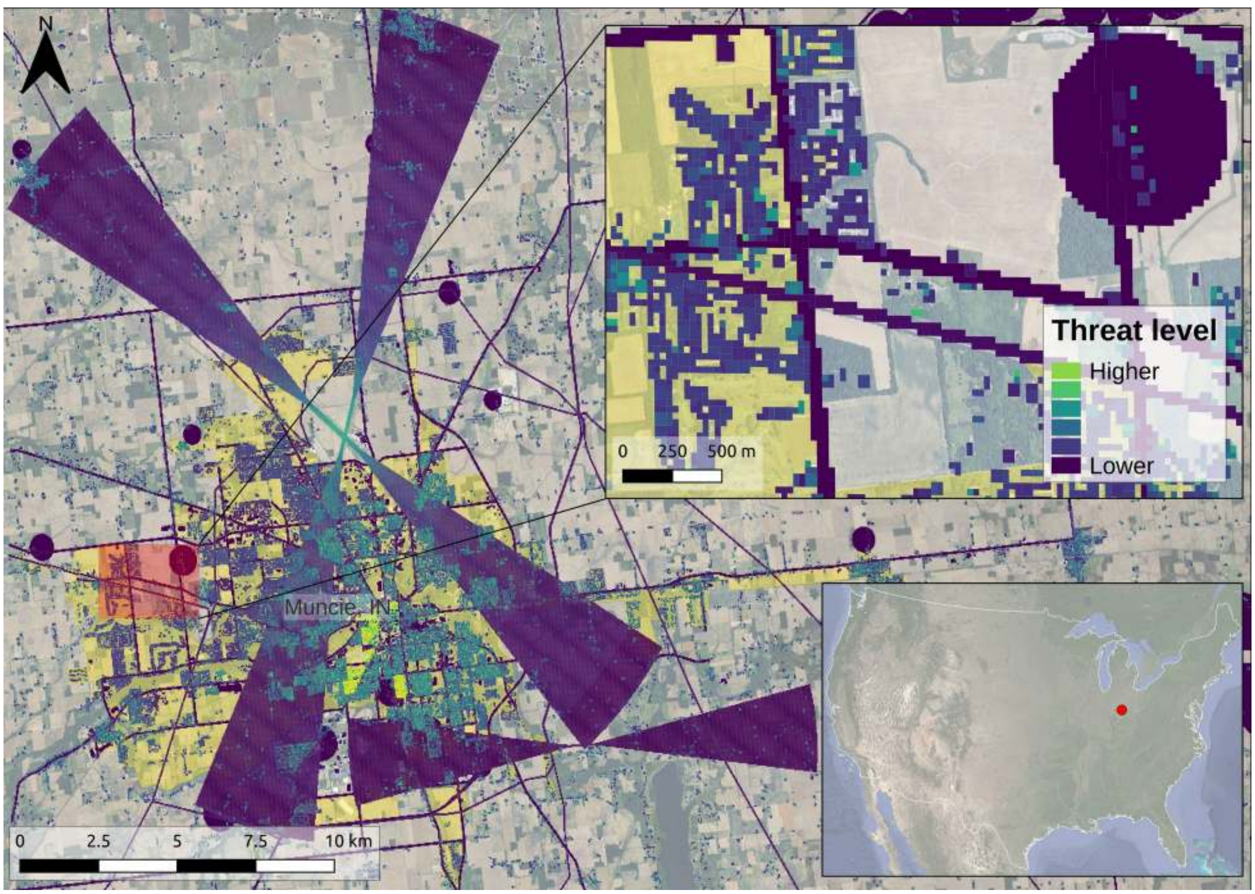

Figure 15. Cumulative-threats map around Muncie, Indiana (semi-transparent yellow polygon), derived by summing the individual-threat maps shown in Figures 4, 6, 8, 10, 12 and 14. *Top-right:* zoomed-in view to an area in west Muncie showing the cumulative threat levels from different threat types. *Bottom-right:* location of Muncie in the United States.

b) Instrumentation:

Multiple versions of the individual- and cumulative-threat maps were created between 2018 and 2025 on different computers. The last version was created on a personal laptop.

- Model: Acer Aspire A515-43
- Memory: 16.0 GiB
- Processor: AMD® Ryzen 7 3700u with radeon vega mobile gfx×8
- Operative system: Ubuntu 22.04.5 LTS, 64-bit

4. Project personnel:

a) Sergio A. Cabrera-Cruz. Unidad de Servicios Profesionales Altamente Especializados, Instituto de Ecología A. C., Xalapa, Veracruz, Mexico

b) Emily B. Cohen. University of Maryland Center for Environmental Science, Appalachian Laboratory, Frostburg, Maryland, United States.

c) Scott R. Loss. Department of Natural Resource Ecology and Management, Oklahoma State University, Stillwater, Oklahoma, United States.

d) Jeffrey J. Buler. Department of Entomology and Wildlife Ecology, University of Delaware, Newark, Delaware, United States.

CLASS III. DATA SET STATUS AND ACCESSIBILITY

A. Status

1. **Latest update:** 4 – 9 December 2025

2. **Latest archive date:** 9 December 2025

3. **Metadata status:** 15 May 2026; metadata are complete and up-to-date.

4. **Data verification:** December 2025.

B. Accessibility

1. **Storage location and medium:** The dataset is available as Supporting Information to this Data Paper publication. A digital version of the dataset is available on Figshare:

   a. Cabrera-Cruz SA, Loss SR, Buler JJ, Cohen EB. YEAR. *Threatscapes for the aeroconservation of birds*: dataset. Data are available in Figshare; DOI: [URL to be added at data paper proof stage].

2. **Contact persons:**

   a. Sergio A. Cabrera-Cruz; sergio.cabrera[at]inecol[dot]mx

   b. Emily B. Cohen; emily.cohen[at]umces[dot]edu

3. **Copyright restrictions:** None.

4. **Proprietary restrictions:** None.

   a. **Release date:** When data paper is published.

b. **Citation:** Please cite this paper when using these data, or a subset of these data, for publication.

c. **Disclaimer(s):**

1. The threatscape maps were built to represent the broad-scale distribution and potential magnitude of impact of bird collision-specific threats, and not actual estimates of expected mortality in any given location.

2. All threatscapes are meant to represent threats to birds over land only, but risk areas associated with airport runways near coastlines may extend over water.

3. The threatscapes were created using geospatial data that was publicly available at the time of creation of each layer. Not all of the geospatial data used to create risk areas was collected in the same year, and the datasets themselves have different years of origin.

5. **Costs:** None.

Class IV. Data structural descriptors

A. Data set file

1. **Identity:**

a. individual_threatscapes.zip:

1. The names of the files contained in this .zip folder indicate the name of the State (49 possible names, in lower case), the threat type (6 possible names, in lower case), and the suffix "_threat_map.tif" with the following structure: statename_threatname_threat_map.tif
2. Example filenames:
    a. alabama_aviation_threat_map.tif
    b. georgia_buildings_threat_map.tif
    c. iowa_comm_towers_threat_map.tif
    d. maryland_power_lines_threat_map.tif
    e. new_jersey_roads_threat_map.tif
    f. ohio_wind_turbines_threat_map.tif

b. cumulative_threatscapes.zip

1. Names of files contained in this .zip folder indicate the name of the State (49 possible names, in lower case), followed by the suffix "_threatscape.tif".
    a. Example filenames
        i. california_threatscape.tif
        ii. district_of_columbia_threatscape.tif
        iii. south_dakota_threatscape.tif

2. **Size:**

   a. individual_threatscapes.zip

      1. Contains 285 files in raster format (.tif) ranging in size from 1.7 kB to 220.6 MB.

      2. Total size of zip folder: 8 GB.

   b. cumulative_threatscapes.zip

      1. Contains 49 files in raster format (.tif) ranging in size from 4.6 MB to 608.0 MB.

      2. Total size of zip folder: 7.1 GB.

3. **Format and storage mode:**

   a. GeoTIFF raster files in .tif format with LZW compression and Albers Conical Equal Area projection.

4. **Header information:** None.

5. **Alphanumeric attributes:** N/A

6. **Special characters/fields:** N/A

7. **Authentication procedures:** N/A

B. Variable information

1. **Variable identity:** N/A

2. **Variable definition:** N/A.

3. **Units of measurement:** unitless.

4. **Data type**

   a. Storage type: Float64 - Sixty four bit floating point

   b. List and definition of variable codes: N/A

   c. Range for numeric values: Pixel values in each raster vary by threat type, their potential impact on birds, number of threats present in each state, and on their overlap.

      1. individual_threatscapes.zip: Minimum value in all raster files is 0. Maximum values range from 0.000005 to 100.

      2. cumulative_threatscapes.zip: Minimum value in all raster files is 0. Maximum values range from 1.91 to 87.72 (rounded to two digits).

   d. Missing value codes:

      1. individual_threatscapes.zip: No missing values present. Areas free of bird-collision threats received a value of 0 (zero).

      2. cumulative_threatscapes.zip: No missing values present. Areas free of bird-collision threats received a value of 0 (zero).

   e. Precision: 15 – 17 significant digits.

5. **Data format**

a. Spatial dimension of rasters, including number of raster columns and rows, vary by state, depending on the state's geographic extent.

C. **Data anomalies:** Some building footprints around the Aberdeen Proving Ground in northeastern Maryland are over water (Fig. 16). We traced this issue back to the geojson file with building footprints used to map the distribution of this threat (Microsoft 2018). All threatscapes are meant to represent threats to birds over land only.

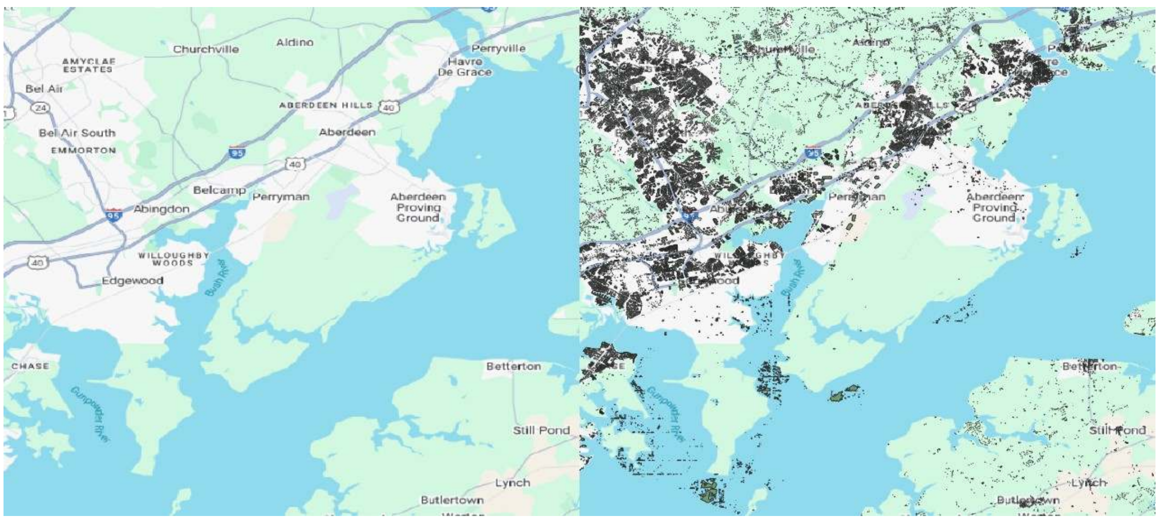

Figure 16. Google maps view around the Aberdeen Proving Ground in northeastern Maryland (left), with building footprints over land and water (right) from the geojson file downloaded from (Microsoft 2018).

CLASS V. SUPPLEMENTAL DESCRIPTORS

A. Data acquisition

1. **Data forms or acquisition methods:** N/A.

2. **Location of completed data forms:** N/A

3. **Data entry verification procedures:** N/A

B. Quality assurance/quality control procedures: Spatial data with the distribution of threats were obtained from authoritative sources. Bird mortality estimates assigned to each threat type, and factors affecting their variability, were obtained from peer-reviewed works. All values expressed in the threatscapes should only be interpreted as indices of potential threat impact on birds, not as spatially-explicit mortality estimates.

C. Related materials: See subsection *3. Research methods*, under section *B. Specific subproject description* of *CLASS II. RESEARCH ORIGIN DESCRIPTORS* for the details of the public geospatial data with the distribution of threats.

D. Computer programs and data-processing algorithms: All data was processed using multiple packages (Table 5) in R (R Core Team 2025) through RStudio (Posit team 2024).

Table 5. List of R packages used to create the threatscapes. Except where indicated, references correspond to current package versions, but previous versions may have been used throughout the years. References were extracted with the R package 'grateful'(Rodriguez-Sanchez and Jackson 2025).

Package	**Reference**
beepr	Bååth (2024)
exactextractr	Baston (2023)
rgdal*	Bivand et al. (2019)
geojsonsf	Cooley (2022)

Package	Reference
gdalUtils*	Greenberg and Mattiuzzi (2015)
geosphere	Hijmans (2024)
raster	Hijmans (2025a)
terra	Hijmans (2025b)
sf	Pebesma (2018) Pebesma and Bivand (2023)
sp	Pebesma and Bivand (2005) Bivand et al. (2013)
tigris	Walker (2025)
tidyverse	Wickham et al. (2019)
devtools	Wickham et al. (2022)
scales	Wickham et al. (2025)
disk.frame	ZJ (2023)

*References correspond to legacy versions of these packages.

E. Archiving

1. **Archival procedures:** Data will be maintained and updated in the Figshare repository.

2. **Redundant archival sites:** A copy of the data will be stored locally by the originators.

F. Publications and results:

- Cabrera-Cruz SA, Loss SR, Buler JJ, Cohen EB. 2022. A threatscape for the aeroconservation of migratory birds. Oral presentation (27June 2022). World Biodiversity Forum 2022. Davos, Switzerland.

G. History of data set usage

1. **Data request history:**

    - Claire E. Nemes. 2024. The cumulative-threat map for the state of Maryland was used in combination with bird densities derived from weather surveillance radar data to identify and map spring and fall landbird migration stopover hotspots across the state. The authors developed specific recommendations for state biologists and other conservation practitioners to promote conservation of stopover habitat and reduce hazards to migrating landbirds, tailored to the species, habitats, and stopover hotspots in each region of the state. This information was incorporated into Maryland's 2025 State Wildlife Action Plan revision.

2. **Data set update history:** N/A

3. **Review history:** N/A

4. **Questions and comments from secondary users:**

    i. Questionable or unusual data discovered by secondary users: None.

ii. Limitations or problems encountered in specific applications of data: According to the secondary user mentioned above and for their specific use, the biggest challenge (with the cumulative-threat map of Maryland) was deciding on meaningful threshold values in order to categorize the level of risk in a given pixel. From a research perspective, the continuously-valued threat index is more interesting and displays more nuance than a categorical classification of threat levels, but it is complicated to quickly identify where the "greatest" hazards / "riskiest" areas occur. From the perspective of a conservation manager trying to identify conflict areas, it will be valuable to convert the threatscape into a categorical "threat hotspot" layer.

    The individual-threat maps have not been used, but those should provide a good understanding of threat levels for every threat type in each state.

iii. Unresolved questions or comments: None.

LITERATURE CITATIONS

Able, K. P. 1977. The flight behaviour of individual passerine nocturnal migrants: a tracking radar study. Animal Behaviour 25:924–935.

APLIC. 2012. (Avian Power Line Interaction Committee). Reducing avian collisions with power lines: the state of the art in 2012. Page 159. Edison Electric Institute and APLIC, Washington, D.C.

Bååth, R. 2024. beepr: Easily Play Notification Sounds on any Platform.

Baston, D. 2023. exactextractr: Fast Extraction from Raster Datasets using Polygons.

Bernardino, J., K. Bevanger, R. Barrientos, J. F. Dwyer, A. T. Marques, R. C. Martins, J. M. Shaw, J. P. Silva, and F. Moreira. 2018. Bird collisions with power lines: State of the art and priority areas for research. Biological Conservation 222:1–13.

Bivand, R., T. Keitt, B. Rowlingson, E. Pebesma, M. Sumner, R. Hijmans, and others. 2019. rgdal: Bindings for the geospatial data abstraction library. R package version 1.

Bivand, R. S., E. Pebesma, and V. Gomez-Rubio. 2013. Applied spatial data analysis with R, Second edition. Springer, NY.

Cooley, D. 2022. geojsonsf: GeoJSON to Simple Feature Converter.

Coues, E. 1876. The Destruction of Birds by Telegraph Wire. The American Naturalist 10:734–736.

Davy, C. M., A. T. Ford, and K. C. Fraser. 2017. Aeroconservation for the Fragmented Skies. Conservation Letters 10:773–780.

Diehl, R. H. 2013. The airspace is habitat. Trends in Ecology & Evolution 28:377–379.

Diehl, R. H., A. C. Peterson, R. T. Bolus, and D. H. Johnson. 2017. Extending the habitat concept to the airspace. Pages 47–69 *in* P. B. Chilson, W. F. Frick, J. F. Kelly, and F. Liechti, editors. Aeroecology. Springer International Publishing, Cham.

Dolbeer, R. A. 2006. Height distribution of birds recorded by collisions with civil aircraft. Journal of Wildlife Management 70:1345–1350.

Dolbeer, R. A., and M. J. Begier. 2019. Wildlife strikes to civil aircraft in the United States, 1990–2017. 106 pages. U.S. Department of Transportation, Federal Aviation Administration, U.S. Department of Agriculture, Wildlife Services, Washington D.C.

Dolbeer, R. A., M. J. Begier, P. R. Miller, J. R. Weller, A. L. Anderson, and W. Major. 2025. Wildlife strikes to civil aircraft in the United States, 1990–2024. 133 pages. U.S. Department of Transportation, Federal Aviation Administration, U.S. Department of Agriculture, Wildlife Services, Washington D.C.

Ellis, E. C., and N. Ramankutty. 2008. Putting people in the map: Anthropogenic biomes of the world. Frontiers in Ecology and the Environment 6:439–447.

Elmore, J. A., S. B. Hager, B. J. Cosentino, T. J. O'Connell, C. S. Riding, M. L. Anderson, M. H. Bakermans, T. J. Boves, D. Brandes, E. M. Butler, M. W. Butler, N. L. Cagle, R. Calderón-Parra, A. P. Capparella, A. Chen, K. Cipollini, A. A. T. Conkey, T. A. Contreras, R. I. Cooper, C. E. Corbin, R. L. Curry, J. J. Dosch, K. L. Dyson, E. E. Fraser,

R. A. Furbush, N. D. G. Hagemeyer, K. N. Hopfensperger, D. Klem, E. A. Lago, A. S. Lahey, C. S. Machtans, J. M. Madosky, T. J. Maness, K. J. McKay, S. B. Menke, N. Ocampo-Peñuela, R. Ortega-Álvarez, A. L. Pitt, A. Puga-Caballero, J. E. Quinn, A. M. Roth, R. T. Schmitz, J. L. Schnurr, M. E. Simmons, A. D. Smith, C. W. Varian-Ramos, E. L. Walters, L. A. Walters, J. T. Weir, K. Winnett-Murray, I. Zuria, J. Vigliotti, and S. R. Loss. 2021. Correlates of bird collisions with buildings across three North American countries. Conservation Biology 35:654–665.

Emerson, W. O. 1904. Destruction of Birds by Wires. The Condor 6:37–38.

FAA. 2023a. (Federal Aviation Administration) Part 139 Airport Certification. https://www.faa.gov/airports/airport_safety/part139_cert.

FAA. 2023b. (Federal Aviation Administration) Airport Data and Information Portal. Advanced Facility Search. https://adip.faa.gov/agis/public/#/airportSearch/advanced.

FAA. 2023c. (Federal Aviation Administration) Airport Categories. https://www.faa.gov/airports/planning_capacity/categories.

FAA and USDOT. 2016. Airport Traffic Patterns. Page Airplane Flying Handbook (FAA-H-8083-3B). Federal Aviation Administration, US Department of Transportation, Oklahoma City, OK.

Falcone, J. A. 2016. U.S. national categorical mapping of building heights by block group from Shuttle Radar Topography Mission data. U.S. Geological Survey.

Fink, D., T. Auer, A. Johnston, M. Strimas-Mackey, S. Ligocki, O. Robinson, W. Hochanka, L. Jaromczyk, A. Rodewald, C. Wood, I. Davies, and A. Spencer. 2022. eBird Status and Trends, Data Version: 2021; Released: 2022. Cornell Lab of Ornithology, Ithaca, NY.

Gehring, J., P. Kerlinger, and A. M. Manville. 2009. Communication towers, lights, and birds: successful methods of reducing the frequency of avian collisions. Ecological Applications 19:505–514.

Greenberg, J. A., and M. Mattiuzzi. 2015. gdalUtils: wrappers for the geospatial data abstraction library (GDAL) utilities. R package version 2.

Hager, S. B., B. J. Cosentino, M. A. Aguilar-Gómez, M. L. Anderson, M. Bakermans, T. J. Boves, D. Brandes, M. W. Butler, E. M. Butler, N. L. Cagle, R. Calderón-Parra, A. P. Capparella, A. Chen, K. Cipollini, A. A. T. Conkey, T. A. Contreras, R. I. Cooper, C. E. Corbin, R. L. Curry, J. J. Dosch, M. G. Drew, K. Dyson, C. Foster, C. D. Francis, E. Fraser, R. Furbush, N. D. G. Hagemeyer, K. N. Hopfensperger, D. Klem, E. Lago, A. Lahey, K. Lamp, G. Lewis, S. R. Loss, C. S. Machtans, J. Madosky, T. J. Maness, K. J. McKay, S. B. Menke, K. E. Muma, N. Ocampo-Peñuela, T. J. O’Connell, R. Ortega-Álvarez, A. L. Pitt, A. L. Puga-Caballero, J. E. Quinn, C. W. Varian-Ramos, C. S. Riding, A. M. Roth, P. G. Saenger, R. T. Schmitz, J. Schnurr, M. Simmons, A. D. Smith, D. R. Sokoloski, J. Vigliotti, E. L. Walters, L. A. Walters, J. T. Weir, K. Winnett-Murray, J. C. Withey, and I. Zuria. 2017. Continent-wide analysis of how urbanization affects bird-window collision mortality in North America. Biological Conservation 212:209–215.

Hijmans, R. J. 2024. geosphere: Spherical Trigonometry.

Hijmans, R. J. 2025a. raster: Geographic Data Analysis and Modeling.

Hijmans, R. J. 2025b. terra: Spatial Data Analysis.

Hoen, B., J. E. Diffendorfer, J. Rand, L. A. Kramer, C. P. Garrity, and H. Hunt. 2018. United states wind turbine database. U.S. Geological Survey.

Homer, C. G., J. A. Fry, and C. A. Barnes. 2012. The National Land Cover Database. Page The National Land Cover Database. USGS Numbered Series, U.S. Geological Survey, Reston, VA.

Johnston, A., A. D. Rodewald, M. Strimas-Mackey, T. Auer, W. M. Hochachka, A. N. Stillman, C. L. Davis, V. Ruiz-Gutierrez, A. M. Dokter, E. T. Miller, O. Robinson, S. Ligocki, L. O. Jaromczyk, C. Crowley, C. L. Wood, and D. Fink. 2025. North American bird declines are greatest where species are most abundant. Science 388:532–537.

Kessler, A. 2017, February 9. Gone with the wind: When Crotched Mountain had a wind farm. Monadnock Ledger-Transcript.

Klem, D. 1989. Bird: Window Collisions. The Wilson Bulletin 101:606–620.

Klem, D. 2025. Bird-window collisions: a critical review. The Wilson Journal of Ornithology 0:1–31.

Korpach, A. M., C. J. Garroway, A. M. Mills, V. von Zuben, C. M. Davy, and K. C. Fraser. 2022. Urbanization and artificial light at night reduce the functional connectivity of migratory aerial habitat. Ecography 2022:e05581.

Lambertucci, S. A., E. L. C. Shepard, and R. P. Wilson. 2015. Human-wildlife conflicts in a crowded airspace. Science 348:502–504.

Legagneux, P., and S. Ducatez. 2013. European birds adjust their flight initiation distance to road speed limits. Biology Letters 9:20130417.

Leu, M., S. E. Hanser, and S. T. Knick. 2008. The human footprint in the West: A large-scale analysis of anthropogenic impacts. Ecological Applications 18:1119–1139.

Li, X., Y. Zhou, M. Zhao, and X. Zhao. 2020. A harmonized global nighttime light dataset 1992–2018. Scientific Data 7:168.

Longcore, T., C. Rich, P. Mineau, B. MacDonald, D. G. Bert, L. M. Sullivan, E. Mutrie, S. A. G. Jr, M. L. Avery, R. L. Crawford, A. M. M. Ii, E. R. Travis, and D. Drake. 2012. An estimate of avian mortality at communication towers in the United States and Canada. PLOS ONE 7:e34025.

Loss, S. R., T. Will, S. S. Loss, and P. P. Marra. 2014a. Bird–building collisions in the United States: Estimates of annual mortality and species vulnerability. The Condor 116:8–23.

Loss, S. R., T. Will, and P. P. Marra. 2013. Estimates of bird collision mortality at wind facilities in the contiguous United States. Biological Conservation 168:201–209.

Loss, S. R., T. Will, and P. P. Marra. 2014b. Estimation of bird-vehicle collision mortality on U.S. roads. The Journal of Wildlife Management 78:763–771.

Loss, S. R., T. Will, and P. P. Marra. 2014c. Refining estimates of bird collision and electrocution mortality at power lines in the United States. PLOS ONE 9:e101565.

Loss, S. R., T. Will, and P. P. Marra. 2015. Direct mortality of birds from anthropogenic causes. Annual Review of Ecology, Evolution, and Systematics 46:99–120.

Martin, G. R., and J. M. Shaw. 2010. Bird collisions with power lines: Failing to see the way ahead? Biological Conservation 143:2695–2702.

McKee, J., P. Shaw, A. Dekker, and K. Patrick. 2016. Approaches to Wildlife Management in Aviation. Pages 465–488 *in* F. M. Angelici, editor. Problematic Wildlife: A Cross-Disciplinary Approach. Springer International Publishing, Cham.

Metz, I. C., J. Ellerbroek, T. Mühlhausen, D. Kügler, and J. M. Hoekstra. 2020. The Bird Strike Challenge. Aerospace 7:26.

Microsoft. 2018. US Building Footprints. Microsoft.

Nemes, C., S. A. Cabrera-Cruz, M. Anderson, L. W. DeGroote, J. G. DeSimone, M. Massa, and E. B. Cohen. 2023. More than mortality: Consequences of human activity on migrating birds extend beyond direct mortality. Ornithological Applications:duad020.

Nilsson, C., J. Shamoun-Baranes, D. A. Satterfield, S. Sjöberg, and E. B. Cohen. 2025. Animal niches in the airspace. Trends in Ecology & Evolution 0.

Pebesma, E. 2018. Simple Features for R: Standardized Support for Spatial Vector Data. The R Journal 10:439–446.

Pebesma, E., and R. Bivand. 2023. Spatial Data Science: With applications in R. Chapman and Hall/CRC.

Pebesma, E. J., and R. Bivand. 2005. Classes and methods for spatial data in R. R News 5:9–13.

Posit team. 2024. RStudio: Integrated Development Environment for R. Posit Software, PBC, Boston, MA.

QGIS Development Team. 2025. QGIS Geographic Information System. Open Source Geospatial Foundation Project.

R Core Team. 2025. R: A Language and Environment for Statistical Computing. R Foundation for Statistical Computing, Vienna, Austria.

R Development Core Team. 2024. R: A language and environment for statistical computing (v. 4.4.2). R Foundation for Statistical Computing, Vienna, Austria.

Rand, J. T., L. A. Kramer, C. P. Garrity, B. D. Hoen, J. E. Diffendorfer, H. E. Hunt, and M. Spears. 2020. A continuously updated, geospatially rectified database of utility-scale wind turbines in the United States. Scientific Data 7:15.

Rodriguez-Sanchez, F., and C. P. Jackson. 2025. grateful: Facilitate citation of R packages.

Rogers, S. E., B. W. Cornaby, C. W. Rodman, P. R. Sticksel, and D. A. Tolle. 1977. Environmental studies related to the operation of wind energy conversion systems. Final report. Page 108. Battelle Columbus Labs., OH (USA), Columbus, Ohio.

Rosenberg, K. V., A. M. Dokter, P. J. Blancher, J. R. Sauer, A. C. Smith, P. A. Smith, J. C. Stanton, A. Panjabi, L. Helft, M. Parr, and P. P. Marra. 2019. Decline of the North American avifauna. Science 366:120–124.

Sodhi, N. S. 2002. Competition in the Air: Birds Versus Aircraft. The Auk 119:587–595.

Soldatini, C., V. Georgalas, P. Torricelli, and Y. V. Albores-Barajas. 2010. An ecological approach to birdstrike risk analysis. European Journal of Wildlife Research 56:623–632.

Spiker, C. J. 1927. Feathered Victims of the Automobile. Wilson Bulletin 39:11–12.

Stoner, D. 1925. The Toll of the Automobile. Science 61:56–57.

Stoner, D. 1936. Wildlife Casualties on the Highways. Wilson Bulletin 48:276–283.

Townsend, C. W. 1931. Tragedies among yellow-billed cuckoos. The Auk 48:42.

USDOT BTS. 2023. (U.S. Department of Transportation: ArcGIS Online). Runway Lines. https://data-usdot.opendata.arcgis.com/datasets/runway-lines.

USDOT FHWA. 2000. (US Department of Transportation Federal Highway Administration). Road function classifications. USDOT FHWA.

USDT FHA. 2014. (U.S. Department of Transportation. Federal Highway Administration). Highway Finance Data Collection. Our Nation's Highways: 2011. https://www.fhwa.dot.gov/policyinformation/pubs/hf/pl11028/chapter1.cfm.

Van Doren, B. M., D. E. Willard, M. Hennen, K. G. Horton, E. F. Stuber, D. Sheldon, A. H. Sivakumar, J. Wang, A. Farnsworth, and B. M. Winger. 2021. Drivers of fatal bird collisions in an urban center. Proceedings of the National Academy of Sciences 118:e2101666118.

Ventana Wildlife Society. 2009. Evaluating diverter effectiveness in reducing avian collisions with distribution lines at San Luis National Wildlife Refuge Complex, Merced County, California. California Energy Commission, Public Interest Energy Research (PIER) Program, Sacramento, California.

Walker, K. 2025. tigris: Load Census TIGER/Line Shapefiles.

Walter, W. D., J. W. Fischer, J. S. Humphrey, T. S. Daughtery, M. P. Milleson, E. A. Tillman, and M. L. Avery. 2012. Using three-dimensional flight patterns at airfields to identify hotspots for avian–aircraft collisions. Applied Geography 35:53–59.

White, F. B. 1927. Birds and Motor Cars. The Auk 44:265–266.

Wickham, H., M. Averick, J. Bryan, W. Chang, L. D. McGowan, R. François, G. Grolemund, A. Hayes, L. Henry, J. Hester, M. Kuhn, T. L. Pedersen, E. Miller, S. M. Bache, K. Müller, J. Ooms, D. Robinson, D. P. Seidel, V. Spinu, K. Takahashi, D. Vaughan, C. Wilke, K. Woo, and H. Yutani. 2019. Welcome to the tidyverse. Journal of Open Source Software 4:1686.

Wickham, H., J. Hester, W. Chang, and J. Bryan. 2022. devtools: Tools to Make Developing R Packages Easier.

Wickham, H., T. L. Pedersen, and D. Seidel. 2025. scales: Scale Functions for Visualization.

Wind Energy Center. 2021. Wind Energy Center Alumni. https://www.umass.edu/windenergy/about/history/alumni.

Winger, B. M., B. C. Weeks, A. Farnsworth, A. W. Jones, M. Hennen, and D. E. Willard. 2019. Nocturnal flight-calling behaviour predicts vulnerability to artificial light in migratory birds. Proceedings of the Royal Society B: Biological Sciences 286:20190364.

ZJ, D. 2023. disk.frame: Larger-than-RAM Disk-Based Data Manipulation Framework.